Review

Screen-Printed Electrodes: Fabrication, Modification, and Biosensing Applications

Giti Paimard [1,*], Ehsan Ghasali [2] and Mireia Baeza [3,*]

1 School of Ophthalmology and Optometry, School of Biomedical Engineering, Wenzhou Medical University, Wenzhou 325027, China
2 College of Geography and Environmental Sciences, Zhejiang Normal University, Jinhua 321004, China
3 GENOCOV Research Group, Department of Chemistry, Faculty of Science, Building C-Nord, Universitat Autònoma de Barcelona, Carrer dels Til·lers, 08193 Bellaterra, Spain
* Correspondence: giti.paimard@wmu.edu.cn (G.P.); mariadelmar.baeza@uab.cat (M.B.)

Abstract: As electrochemical measuring instruments, screen-printed electrodes (SPEs) are constructed via a technology called thick film deposition onto plastic or ceramic substrates, allowing for simple, inexpensive, and rapid on-site analysis with high reproducibility, sensitivity, and accuracy. Numerous substances such as gold, silver, platinum, and carbon are applied for electrode construction, enabling the analyst to design the best device based on its purpose to determine an analyte's selectivity and sensitivity. Thus, in the current review, we report the latest results and analyses conducted over the past eight years (2015–2022) on the expansion of SPE electrochemical biosensors, including aptasensors, immunosensors, DNA sensors, and enzymatic biosensors. Such expansion has resulted in new possibilities for the identification, distinction, and quantification of biocompounds, drugs, enzymes, etc. Therefore, in this paper, we review the role of different nanomaterials in manufacturing on-screen electrode methods as well as strategies for the future stable diagnosis of biorecognition elements.

Keywords: screen-printed electrodes (SPEs); nanomaterials; biosensor; DNA sensor; aptasensor; immunosensor; enzymatic biosensors

1. Introduction

Analytical chemists are typically challenged with devising methods capable of accomplishing rapid in situ analyses due to the fact that such methods are mainly expected to be accurate and sensitive while being able to detect and measure different materials with various attributes in "real-life" samples. The existing commercial laboratory tests have been reported as being complex and costly, and thus are used less for in situ and point-of-care solutions intended for quality control, environmental surveillance, and healthcare monitoring [1,2]. Over the years, sensors based on screen-printed electrodes (SPEs) have emerged as one of the main branches of electrochemical research for rapid, specific, portable, sensitive, low-cost, and precise analyses, and have been claimed as having innovative applications [1,3,4]. A key driving force behind these historic developments was the realization that screen printing can be much cheaper than traditional manufacturing methods [5]. In the microelectronics industry, for the past three decades screen printing has been proposed for the mass production of reproducible, cheap, reliable, single-use sensors as an on-site monitoring technique [1]. On the one hand, SPEs allow the fabrication of large numbers of carbon electrodes in reproducible, low-cost, and disposable formats, also combining functionalized chemicals. On the other hand, SPEs are used in many electrochemistry fields, especially in measurements of chemical and biochemical compounds and microelectronics, as well as in the conversion and storage of energy. Moreover, these electrodes are applied in flexible electronics, a rapidly evolving technology for printing electronic devices directly on flexible plastic materials such as polycarbonate, polyamide, and polyetheretherketone. All the carbon forms, especially graphite, activated carbon,

and carbon black, have the broadest applications for deposition onto these electrodes. In comparison with other electrode fabrication methods, SPEs have the advantage of easy control of the electrode's thickness, surface, and composition, and catalysts can be added to the printing ink for easy combination. Moreover, they offer the possibility of experimental statistical validation of the results notwithstanding the existence of duplicate electrodes. Their most noticeable disadvantage is that they are limited to flatbeds [5].

SPEs allow a plurality of tests to be accomplished with low volumes of samples and reagents without pretreatment or keeping of the electrode. These electrodes are often employed for analyses in fields such as agriculture, pharmacy, medicine, the food industry, and the environment [4].

While it is known that SPEs can vary in terms of shape, they can also be made on demand for analysis. Moreover, they come in various forms such as a disc, a ring, or a band. By employing SPEs, not only can calibration be performed, but they are also used for simultaneously and promptly analyzing numerous unknown samples. However, despite the mentioned advantages associated with SPEs, they are incompatible with nonplanar substrates, which remains a disadvantage in terms of limiting the fabrication methodology. As a result, SPEs, which are printed directly onto several flexible and inflexible substrates, must be further developed [6].

In the current research, we compare SPEs' application and performance from 2015 to 2022 as electrochemical biosensors, taking into consideration DNA sensors, aptasensors, immunosensors, and enzymatic biosensors (Figure 1). It is acknowledged that analytical methods for in-field screening and monitoring solutions can be substituted by electrochemical biosensors as long as they are combined with SPEs. This has applications in various fields from the food industry to environmental uses, in addition to forensics and cancer biomarker analysis [2,7]. Bearing this in mind, the latest advancements in SPE-based biosensors are summarized in this paper, along with a discussion of future favorable developments.
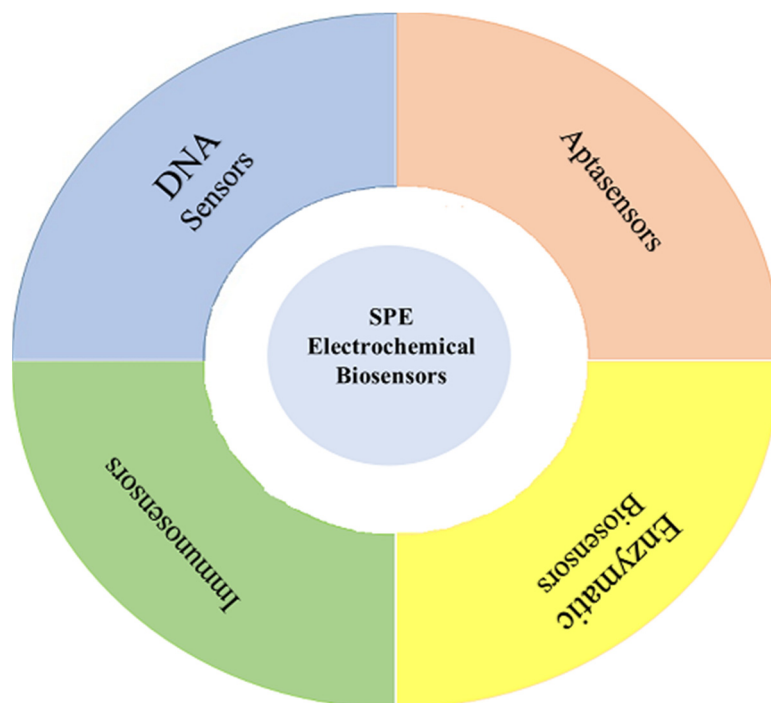

Figure 1. Classification of SPE electrochemical biosensors.

2. SPEs: A Brief Overview

At present, the screen-printing system is a well-established method for electroanalytical instruments' conception with various uses in the biomedical field [8–10], food measurement [11,12], and environmental pollutant detection [6,13,14]. SPEs are often

composed of an electrochemical cell that consists of three electrodes, namely the pseudo reference electrode (RE), counter electrode (CE), and working electrode (WE), which are printed on a solid substrate, as shown in Figure 2 [4].
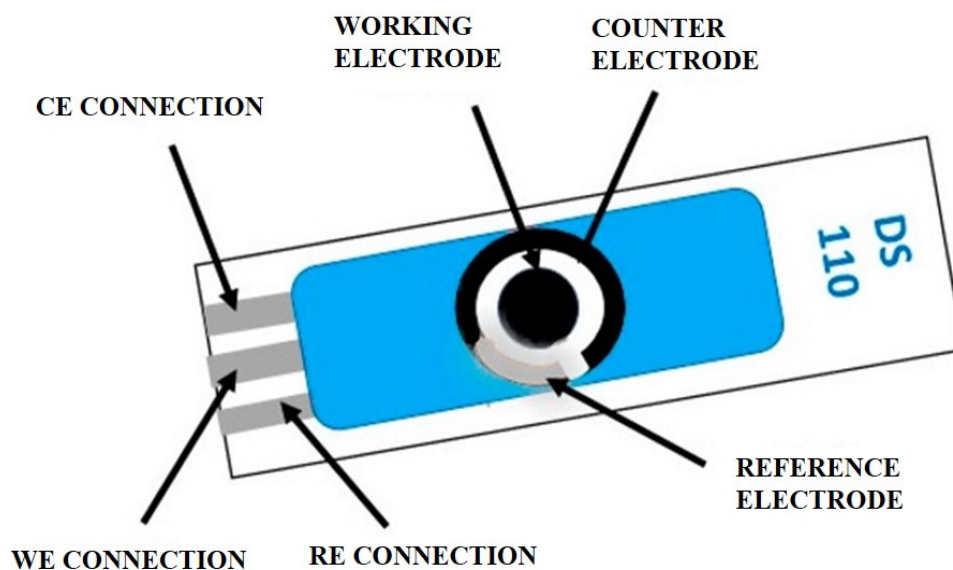

Figure 2. The most common scheme form of an SPE (adapted and reprinted with permission from [4]).

SPE devices appeared in the 1990s and since then they have been increasingly used due to their low price, reproducibility, reliability, and capacity for mass production. It has been shown that SPEs are flexible instruments, appropriate for various configurations, constructed from various substances, and can be modified by different biological substances including synthetic diagnosis elements, DNA, enzymes, and antibodies [9]. As previously mentioned, SPEs as planar devices consist of three electrodes, namely WE, CE, and RE, which are placed on the same substrate such as plastic, ceramic, or textile [8,15,16]. These electrodes have several desirable properties, including simplicity, low cost, the possibility of being made by various substances with flexible selectivity, the consumption of minimal sample volumes of analyte, and minimal waste production. These attractive properties have made these devices applicable to the development of analytical procedures as well as analyte detection, including in clinical [9], pharmaceutical [8,15], environmental [6,17], and microbiology fields [18], in addition to heavy metal ions [19] and liquid (bio) fuel [20] samples. SPEs can be employed as disposable tools owing to their low price and feasibility of mass production. Hence, the usual difficulties of the classical solid electrodes, including surface contamination, passivation of surface, and tedious cleaning procedures, are not present in these electrodes. Despite this, there are some limitations of this method: (1) the reproducibility of these devices is close to or greater than 5%; (2) the high cost of devices due to the application of specific substances for SPE production or analysis of several samples; (3) the device is not changed after each analysis and nonproductive analysis after using automated or mechanized procedures with on-site sample preparation steps and the ones followed by the analysis [21].

2.1. Construction of SPEs

SPEs are constructed by popular industrial printers by the deposition of composite layers onto a flat substrate [2]. Figure 3 exhibits the manufacturing process of these electrodes [22].

Although the screen-printing process was withdrawn from microelectronics manufacturing, the process is applied for the production of SPEs, among other applications. These electrodes suggest the original attributes needed to acquire electrochemical detection platforms in on-site analysis [23].

The published papers have recently acknowledged that most SPEs are constructed with materials from Metrohm DropSens (Oviedo, Spain) or Gamry Instruments (Warminster, PA,

USA). However, there are some producers in China and Europe that are also specialized in the design of tools for electrochemistry evaluations [4].

The construction process of the SPE is rapid and permits the exhaustive and highly reproducible production of single-use electrodes with a small size and low price [23]. Carbon and metallic inks, which are the most common of various inks or pastes (viscous fluid) to print the electrodes [24], are compressed by means of a blade (3–10 Pa at a sheer rate of 230 s^{-1}) using a mesh screen on the substrate (which is often ceramic or plastic such as polyvinylchloride and polycarbonate) [16,25,26]. The mesh screen has a specific template that describes the dimensional attributes of the electrodes [27].

The paste formulation is mostly a commercial mystery because of the overall analytical operation and trading value of manufacturing sensors [28]. The most common inks used in WEs are carbon-containing graphite, fullerene, graphene (Gr), carbon nanotubes (CNTs), etc., and this is due to their favorable properties in electrochemical evaluations, which include their low prices, chemical stability, higher conductivity, facility of modification, broad potential ranges, and lower background currents [8,29–31]. Conductive metallic inks have also been extensively used along with carbon inks. Moreover, thanks to its resemblance to thiol moieties, Au ink is the most common as it permits easy surface modification with proteins using a self-assembled monolayer (SAM) formation. It is of note that there are other SPEs available, which have a WE crafted using other metallic inks such as silver (Ag), platinum (Pt), or palladium (Pd); nevertheless, their use is uncommon and extendeds only to particular applications. Indeed, it is documented that silver or silver/silver chloride inks are usually applied for RE construction, which is considered as quasi or pseudo RE due to the lack of stability of its potential, contrary to an ideal RE. Hence, as opposed to ideal REs such as the Ag/AgCl electrode, the realistic potential has not been considered to be as precise and reproducible. The ink chemical structure towards the electrochemical aims is significant. The ink formula and structure of SPEs are patented by several companies and are not revealed to users. The composition of the ink can be changed by altering the number of particles loaded, which forcefully affect the electron transfer process and the designed SPEs' performance [7,32–35].

This can be difficult for electrochemical evaluations in which potential control is needed; however, it is not often a problem for detection utilizations. For making CEs, the same inks as for WEs are usually employed. SPEs are diverse because the ink configuration determines the electrode's electrochemical properties. Therefore, SPEs are versatile because various inks are employed and the WE is easily modified. Such alterations are undertaken not only to boost the electroanalytical properties of the SPEs, but also to enhance the recognition element's immobilization. These recognition elements could not only be biological such as DNA, proteins, and the like, but they could be synthetic as well, such as molecularly imprinted polymers [23]. To increase SPEs' conductivity, ink slurries are often pulverized in ball mills. This process produces tiny particles of a conductive carbon called fines with diameters between 1 and 100 nm, which fill electron tunneling gaps between larger particles after printing [36]. Over several years, countless binder–solvent compounds have been tested in screen printing formulas, but only a few have been prosperous and have gained a commercial value. Two different types of thermoplastic and thermosetting polymer binders are widely used, including poly (vinylidene fluoride). The most popular method among electrochemists is to dissolve a thermoplastic polymer in a high-boiling solvent [5].

Adhesives such as ethylene glycol, cellulose acetate, resin, or cyclohexanone are added for attaching the paste to the substrate. Blending the additives may be accomplished to enhance the sensitivity, specificity, and signal-to-noise ratio (S/N). Occasionally, it is documented that with the purpose of augmenting the electrochemical signal for physical or biochemical interactions, the ink possesses silver, platinum powder, or even gold [37].

To summarize, SPE construction involves several steps: (1) the mesh or screen design to define the SPE size and geometry; (2) the choice and provision of the conductive inks and the proper substances for the substrate; (3) thin film fabrication by layer-by-layer (LBL)

deposition for selecting the inks on the substrate; (4) drying with hot air and IR radiation, in addition to curing to solidify the ink. Having covered the electrical circuits by means of an insulating substance, which is executed by adding a distinct drop of the sample (analyte) solution on the SPE surface, the analytical evaluations can be accomplished [6,8].

The pretreatment of SPEs is important to overcome the restricted electron transfer kinetics in it when having an interface with the electrolyte. This happens because these electrodes contain insulator additives to ameliorate the carbon ink adhesion. For activating the SPE edge planes, although several methods have been evaluated to increase the electroactivity of the carbon, electrochemical methods are the most frequently applied. The method of 10 cyclic voltammetry (CV) cycles in phosphate buffer solution (0.05 M) remaining between -0.5 and 2.0 V vs. Ag/AgCl was suggested by Sundaresan's group [38]. Pan's group applied a constant potential (-1.2 V vs. Ag/AgCl) within 20 s so that an electrode would possess a drop of NaOH (0.1 M) [39].
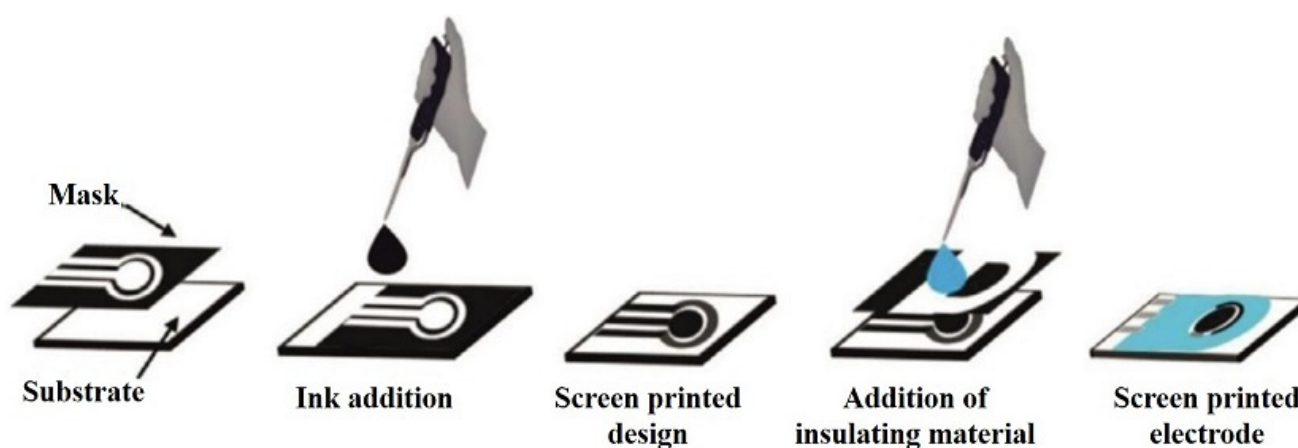

Figure 3. The construction process of SPEs (adapted and reprinted with permission from [2]).

2.2. Methodologies of Modification

SPEs' ability for modification and miniaturization was gradually developed, which later attracted more attention in biomedical and clinical fields. So far, different biosensors have been commercially accessible for many applications in clinical, environmental, and food fields [40]. To improve their analytical properties, several alterations have been applied using different nanomaterials and synthetic distinction substances, which almost yielded prosperous outcomes in many of the experimented instances. Therefore, carbonaceous compounds including carbon black (CB), CNTs, Gr, and metallic NPs (Au and Ag as well as magnetic beads (MBs)), in addition to mediator NPs (cobalt phthalocyanine and Prussian blue) have been used for SPE modification. Nanosubstances can possess identical dimensions of biological diagnosis elements, including proteins and DNA, whose composition can produce synergistic impacts that provide unpredicted profits. The emergent and inspiring actions in nanotechnology progress have strongly influenced investigations in the enzyme biosensor field. The nanomaterial's ability to offer amended electrocatalytic activities and reduce electrode surface deposition makes them beneficial for developing biosensors [41,42]. The electrochemical behavior of nanomodified sensors was evaluated using cyclic voltammetry (CV), electrochemical impedance spectroscopy (EIS), and amperometry to accurately communicate the electrochemical behavior of the sensor by the nature of nanomaterials, and to perceive the impacts of the nanomaterials on the analytical properties [43]. In effect, by making use of nanomaterials, it is highly feasible to enhance the analytical properties such as the sensitivity and selectivity, as well as increase the stability while decreasing the limit of detection (LOD). In addition to these nanomaterials, a plethora of other materials can also be employed. These include polymers and metal oxides in addition to redox mediators with complexing agents and so forth. The easiest method for modification of the SPEs is based on the modifying agent deposition on the WE, which is

supported by the planar nature of the SPE. Accordingly, this could be accomplished with an automated dispenser in a mass production method. Furthermore, the SPEs such as the WE can be altered prior to printing by appending the modifier to the ink. This is fulfilled by means of electrochemical or chemical deposition [44–46].

The electrode surface modification of these tools is often performed by three well-known procedures, as shown in Figure 4. These procedures consist of mixing the ink by the modifier agent, a metallic progressive electrochemical deposition, or nanomaterial drop casting. Prior to ink curing, the initial procedure is performed, which contains further critical parameters. Such parameters mainly include the temperature of the curing in addition to the instructions for mixing. In practice, these must be monitored so that batch reproducibility will be attained [47]. To develop the assay, ink mixing was referred to as the primary method and as appropriate for yielding metalized SPEs. Nonetheless, such a procedure is disadvantaged by NP accumulation, multifaceted ink instructions, and weak reproducibility between batches. The other two procedures are accomplished on their surfaces after electrode procurement, which are thus more appropriate when using commercial SPEs. Drop casting methods provide an appropriate way for SPE modification because modifications are undertaken, having prepared the ink. In practice, the NPs which are deposited onto the surface of the WEs show a highly active surface for the analyte, but aggregation occurs as well. NPs with precisely tailored shapes and sizes can only be obtained using electrodeposition. Potentiostatic methods are more widely used thanks to their applications in traditional three-electrode cells having a well-controlled RE, and their use has been common for several years. However, when working with SPEs, the galvanostatic methods are more effective. Besides, possible changes in the quasi-RE exert no impact on the deposition, which is undertaken under a controlled current, and this offers abilities akin to the nucleation and growth control of metal NPs as potentiostatic methods. Nevertheless, the major problem of this procedure is its large-scale synthesis, since the electron deposition is typically conducted with each sensor individually, while the deposition step is laborious and consuming when considering the preparation of large batches [45].

The mediator's utilization on the electrode surface and the creation of surface oxygen functionalities are considered as additional fundamental characteristics in understanding the SPE reactivity [48]. To obtain more information, it would be better to focus on generating oxygen functionalities as well as edge–plane-like sites via chemical alterations to evaluate some of the significant recent progress made in SPE design. In this field, the application of Gr and CNTs, as popular carbon substances, has changed the range of electroanalysis. The utilization of carbon nanomaterials was illustrated as one of the procedures, both analytically and economically, that can be employed for the fabrication of modified SPEs. Concerning the detection of many targets, the increased electrocatalytic attributes are ascribed to the defect– and edge–plane-like sites on the Gr and CNT surfaces [49,50].

2.3. Applications of SPEs in Electrochemical Biosensing

SP electrochemical biosensors have received attention as analytical devices for agriculture, pharmacy, medicine, and food analysis due to benefits such as their low cost, ease of use, low volumes, and ability to be moved freely and easily [11–13]. Hence, the SP process has considerably helped in the transition from the classic unbearable electrochemical cells to miniaturized and portable electrodes that meet the requirements for on-site analysis [13,51]. However, an SPE, as a typical electrode, such as a glassy carbon electrode or gold disk, is not a strong electrode and its surface is not as ideal as that of a mirror-like polished solid electrode. Yet in recent years, SPEs' benefits in terms of their cost and size led to the enhancement of their application as transducers in biosensing [23].

SPEs fabricated based on sensitive and selective sensors have been used extensively for various analytes in clinical and pharmacy fields. The possibility of making attractive designs for single and multiple analyses even in the absence of biological substances is one of the notable advantages of these sensors. In the field of physiological evaluation, the

activated sensor surface is exposed to the epidermis (oral mucosa in the mouth, stratum corneum, or skin) to distinguish related biomarkers such as glucose [52] and ethanol [53] in various informative biofluids such as tears, saliva, and sweat. The combination of SPEs with simple paper-based microfluidics shows different benefits of electrochemical biosensors' procurement in comparison with traditional analytical tools constructed by other substrates such as polymers, silicon, or glass. The fabricated tools are cheap, have simple construction, and are compatible with different chemical or biochemical utilizations [54]. The high surface area in the cellulose papers offers effective substrates along with SPEs for prototyping new point-of-care detection tools such as microfluidic systems in clinical settings.
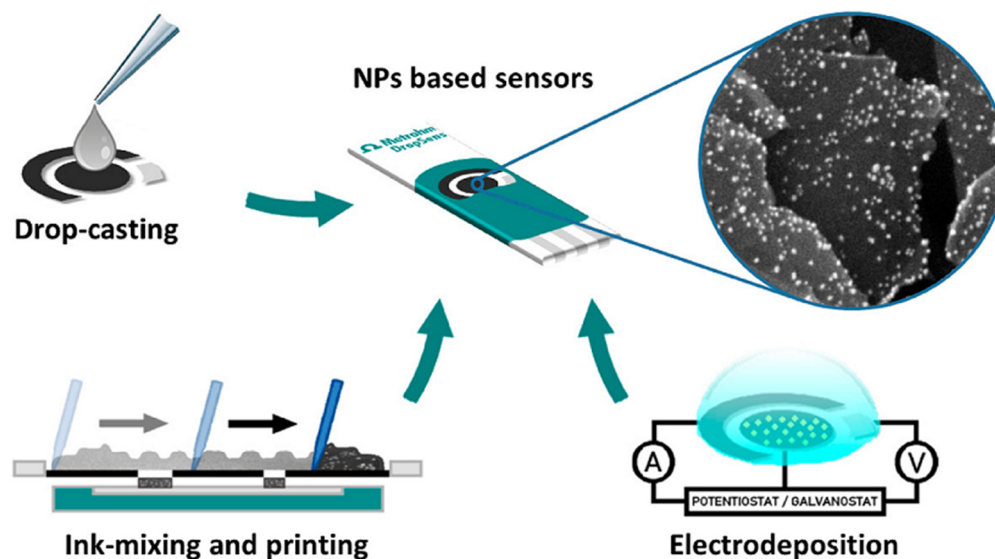

Figure 4. Schematic of the three main procedures for SPE modification using metal NPs (adapted and reprinted with permission from [45]).

An area where SPEs have shown specific communication is in environmental detection. Various samples of paper presented with proper substances, modified with metal NPs or carbon nanostructures both in the absence or presence of special enzymes, have been employed to measure pollutants, including heavy metals and anions [55–58].

3. Biosensors

Biosensors are useful tools for the detection of chemical and biological substances as well as the quantitative or semi-quantitative analytical information use of sensitive detection substances [59,60]. The sensitive, selective, and fast detection of targets is the main purpose of these instruments, which is the aim of the evolution of sensors. The biosensors have a transducer part that converts the biological treatment into a detectable signal. Different biosensors with various biological and biomimetic elements have been recognized which have various transducer parts whose physiochemical application categorizes the sensor as electrochemical, optical, piezoelectric, etc. Miniaturization of electrochemical biosensors based on SPEs has yielded numerous point-of-care tools in the past and is anticipated to soon change real-time detection. SPEs' advancement lies in the possibility to modify these devices with tunable nanocomposites as modifiers to increase the sensor selectivity. Glucose biosensors are known as the most extensively used point-of-care SPE tools based on the electrochemical rule. To enhance the SPE validity, the reply time and availability of the modified SPEs are options that are acquiring great popularity. Few papers are published on unmodified SPE-based biosensors. Graphite ink, CNT ink, and Gr ink are commonly used for the construction of SPEs [61]. This review explores the most promising developments in electrochemical biosensors over the past eight years (2015–2022), including DNA sensors, aptasensors, immunosensors, and enzymatic biosensors.

3.1. DNA Sensors

The utilization of single-use electrodes has acquired many applications within electrochemical DNA sensors. As such, the potential to detect specific DNA sequences has recently been taken into consideration because of their use in various areas, from detecting pathogens to diagnosing genetic maladies [62–64]. The mentioned sensors are currently being expanded and enhanced for extensive types of DNA sequences which cause known ranges of diseases (Epstein–Barr virus, herpes simplex virus, and cytomegalovirus), specified pathogens (*Salmonella* and *E. coli*), and genetic mutations. Moreover, by making use of specific DNA sequences, it has been possible to undertake electrochemical diagnosis of proteins. These proteins include transcription factors or other DNA-binding proteins. Aptamer targets, together with proteins or small molecules, are also among such proteins. In comparison with other procedures such as optical detection, the electrochemical detection of DNA hybridization is associated with numerous considerable merits, including faster response time and lower costs in addition to their suitability for mass production. In this field, single-use electrodes have grown in significance, and these electrochemical chip types have been extensively applied to the construction of DNA sensors.

Since gold-based ink is costlier than the usual carbon-based ink, many of these single-use electrodes make use of gold-based ink because this allows attaining well-arranged gold thiol by DNA whose end is modified with alkane thiols based on SAM. It has been confirmed that the quality of the SAMs gained on the mentioned electrodes will be superior and contribute to attaining higher reproducibility and impressive electron transfer rates. This is nevertheless the case regardless of the SPEs' roughness issues or their surface defects because of the fact that these have been reported to be incomparable with typical gold rod electrodes (distinguished with a high smoother surface area) [65].

Recently, numerous instances have been suggested for DNA and RNA sequences based on electrochemical measurements with single-use electrodes. Table 1 gives the analytical properties as well as the chief characteristics of a few of the recent and characteristic procedures used in biological samples [66–82]. Several instances are discussed below.

Heavy metal ion contamination such as mercury (II) ion (Hg^{2+}) might impose threats not only to the environment but also to human health. In recent years, there has been a growing interest in coordinate interaction among Hg^{2+} and bis-thymine of DNA, where Hg^{2+} is likely to bind two thymines, substituting the imino protons while prompting a conformational change, which relies on the base pairs' sequence. Indeed, such an interaction is distinctive for Hg^{2+}, as revealed in the analysis of other metal ions. Hg^{2+} could be determined with an outstanding degree of selectivity using the DNA biosensors by forming the complex Thymine-Hg-Thymine (T-Hg-T). Tortolini's group developed a simple but reusable electrochemical sensor for determining mercury content through the "signal on" assay mode, in which a polythymine is typically altered in the 3′ position with methylene blue (MB) as the redox probe. Although MB has been mostly utilized as an intercalative probe with the aim of detecting DNA strands' hybridization, it has also been considered as an electrochemical probe for DNA-based biosensors. It is of note that the T–Hg–T complex contributes to the "hairpin-like" folding of an oligonucleotide. As a result, the MB proceeds towards the electrode surface, resulting in a better-quality electronic exchange between the MB and the SPGE; this occurs both for the decreased distance and an upsurge in the faradic current [68].

Immobilization of biomolecules such as DNA on a screen-printed carbon electrode (SPCE) is a challenge, which is why choosing an easy yet efficient approach to electrode surface modification is important. A unique reactive adhesive polymer is typically applied to coat diverse surfaces. This modifies the SPCE with a dopamine (DA) electropolymerization film, and a layer that adheres tightly to the SPCE, thus providing opportunities for further surface modification.

It is to be noted that the equilibrium between quinones in polydopamine (PDA) tends to move in the direction of the latter. This makes the biomolecules' one-step covalent bonding possible, which encompasses amino groups onto PDA-coated substrates via

Michael addition or Schiff base reactions. Meanwhile, the PDA-modified surfaces can resist nonspecific adsorption. In this study, the SPCEs were primarily functionalized with active groups by means of electropolymerization of DA. Afterward, the DNA sensor was acquired through a one-step covalent attachment of the amino-terminated probe DNA onto the PDA-modified SPCE by means of Schiff base reactions which occur in slightly basic pH conditions. Having executed the hybridization of the target DNA to the immobilization probe DNA, the reporter DNA-functionalized gold nanoparticles (AuNPs) were introduced onto the sensor surface by means of sandwich hybridization. DNA bases, particularly adenine sequences, maintain a high adsorption affinity with Au substrates [70].

Fast electrochemical detection of trace Hg^{2+} was reported by Zhang's group, which was based on the "turn-off" reaction between a hairpin DNA probe binding a mismatched target and Hg^{2+} using the $T-Hg^{2+}-T$ coordination formation, which depended on the conjugated hairpin DNA probes with water-soluble and carboxyl-functionalized quaternary Zn–Ag–In–S quantum dots (QDs) on SPGE (Figure 5). The hairpin DNA probe's conformational variation led to a considerable reduction in the electrochemical signal, which could be employed for Hg^{2+} detection. The attained Zn–Ag–In–S QDs depicted high stability in water, illustrating the feasibility of identical electrode surface modification [79].

As a base for a self-powered biosensor, Becker's group utilized an enzymatic biofuel cell which was employed on an SPE. The EBFCs applied the enzymes as biocatalysts with the aim of accomplishing the catalytic change in the substrates employed as an oxidant, fueling two individual electrodes. In practice, the most forthright choice is to use an analyte conversion as a fuel for the EBFC so that there will be the possibility of discriminatorily oxidizing the analyte via a proper enzyme that has been immobilized at the bioanode. Meanwhile, for closing the circuit, a nonlimiting (bio) cathode will be utilized. A bioanode was integrated here with the aim of converting the glucose with pyrroloquinoline quinone (PQQ)-dependent glucose dehydrogenase (GDH) with the BOD-based gas-diffusion bioelectrode on an SPE. Moreover, using a miniaturized agar salt bridge, it was possible to separate the two bioelectrodes. This was undertaken in order to ascertain that assembly occurs optimally in a two-compartment configuration with each electrode. All this demonstrates that the individual electrodes operate optimally, while making it possible to utilize smaller sample quantities [81].

Table 1. DNA SPE biosensors for (bio)compound measurements in various targets.

Sensor Construction	Technique and Method	Detection	Analytical Characteristics	Analyte/Sample	Ref.
ASV-QD DNA assay	The inserted bismuth citrate was simultaneously transformed in situ to bismuth NPs by Pb electrolytic accumulation on the surface of the sensor	ASV	L.R.: 0.1 pM–10 nM LOD: 0.03 pM	Pb (II)/N/A	[66]
SiNWs/AuNPs-SPGE	SiNWs/AuNPs and MB (redox indicator) were used to increase the SPGE conductivity, as well as to produce a suitable site for immobilization and hybridization of the DNA probe	CV/DPV	L.R.: 0.1 pM–100 nM LOD: 1.63 pM	DNA oligomers related to dengue virus/N/A	[67]
Au/polythymine/ MB/SPE	The Hg^{2+} detection was performed with the Thymine–Hg–Thymine (T–Hg–T) complex formation	SWV	L.R.: 0.2–100 nM LOD: 0.1 nM	Hg^{2+} ions/Waters and fishes	[68]
CNF/SPE	The sequence-selective DNA hybridization was performed following the bonding amino miRNA-34a inosine, which substituted the DNA probe at the CNF-SPE surface	EIS (Fe $(CN)_6^{3-/4-}$) /DPV	L.R.: 25–100 µg/mL LOD: 10.98 µg/mL	miRNA-34a target RNA/N/A	[69]

Table 1. *Cont.*

Sensor Construction	Technique and Method	Detection	Analytical Characteristics	Analyte/Sample	Ref.
PDA/SPCE	Covalent immobilization of amino-terminated probe DNA was executed on the surface of the sensor's Schiff base: reaction of the quinones in PDA and the amino group of the probe DNA was based on the sandwich-type hybridization. Finally, the AuNP-labeled reporter DNA was bound onto the sensor's surface to increase the signal	EIS (Fe $(CN)_6^{3-/4-}$)/LSV	L.R.: 1.0–70 pM LOD: 0.3 pM.	Target DNA/N/A	[70]
Au/SH-ssDNA/ MCH/SPGE	The response of this sensor was based on the ion channel mechanism	CV/OSWV	LOD for 280-mer RNA: 1 pM	Specific DNA and RNA sequences derived from Avian Influenza Virus H5N1/N/A	[71]
PMCSPE	MB was employed as the hybridization indicator; the –COOH groups of PBA were reused to immobilize oligonucleotides based on covalent bonding among the –NH$_2$ groups of oligonucleotides and –COOH groups of PBA	DPV	L.R.: 1.0 aM–10 nM and 1 aM–0.1 nM LOD: 0.11 and 0.24 aM	M268T mutation of angiotensinogen gene/human blood samples	[72]
SH-probe/SPGE	The high selectivity of this biosensor in detecting the specific target DNA oligo in the real biological environment of unspecific DNA sequences was due to the considerable variation in the signal of the accumulated hematoxylin, between nonspecific oligos and target DNA oligo	EIS (Fe $(CN)_6^{3-/4-}$)/CV	L.R.: 20 pM–150 nM LOD: 8.5 pM	PAH/N/A	[82]
DNA biosensor	Ebola virus DNA, diagnosable by enzyme-amplified detection	EIS (Fe $(CN)_6^{3-/4-}$)/DPV	N/A	Ebola virus DNA/N/A	[73]
PANI/AuNP/ avidin/SPCE	The sensing mechanism was based on an enzymatic reaction (interaction between HRP enzyme and TMB/H$_2$O$_2$). HRP converted a nonelectroactive substrate into an electroactive substrate	CV	L.R.: 0.001–1000 pM LOD: 0.5 fM	*E. coli*/Urine sample	[74]
DNA/sgRNA/dCas9/ PAMAM/Cys/AuE	A practical, sensitive, and fast impedimetric/capacitive biosensor with CRISPR-dCas9 was modified by sgRNA to assess the most common IDH mutation in glioblastomas	EIS (Fe $(CN)_6^{3-/4-}$)	L.R.: 100–1000 fM LOD: 33.96 fM	Glioblastoma (target mutant DNA)	[75]
ds-DNA/PtNPs/ AgNPs/SPE	Interaction between dsDNA and three anthracyclines: EPI, IDA, and DOX by DPV	DPV	L.R.: 0.3–1.3 ppm for EPI 0.1–1.0 ppm for IDA/DOX LOD: N/A	Interaction between DNA and three intercalating anthracyclines	[76]
DNA/Gold-plated silver and DNA/SPE	An enzyme-amplified electrochemical assay permitted the PIK3CA point-mutations detection	Chronoamperometric	L.R.: 1–100 nM LOD: 10 pM	PIK3CA point-mutation (H1047R)/Plasma	[77]
DNA−MnO$_2$ nanosheets/SPE	ctDNA analysis is performed by controlling the adsorption and desorption of DNA strands on MnO$_2$ nanosheets	SWV	L.R.: 1 fM–1 nM LOD: 0.1 fM	ctDNA/Fetal bovine serum samples	[78]
HP-QDs-SPGE	The "turn-off" reaction of a hairpin DNA probe binds with a mismatched target and Hg^{2+} through the formation of T–Hg^{2+}–T coordination	CV/DPV	L.R.: 10 pM–1 mM LOD: 0.11 pM	Hg^{2+} ions/Deionized water, tap water, groundwater, and urine samples	[79]

Table 1. *Cont.*

Sensor Construction	Technique and Method	Detection	Analytical Characteristics	Analyte/Sample	Ref.
$Fe_3O_4@SiO_2/$ DABCO/SPE	The DPV signals of the hemin reduction and the guanine oxidation as an electrochemical indicator with indirect and direct methods, respectively, were applied to detect the hybridization process	DPV	L.R.: 10 pM–2 μM for guanine oxidation 7.5 pM–2 μM for hemin reduction LOD: 8 pM for guanine oxidation 6.4 pM for hemin reduction	Short-sequence DNA of PCa/N/A	[80]
Glucose/O_2 biofuel cell	The biofuel cell was constructed by coupling a biocathode for O_2 transformation based on a BOD-modified gas diffusion electrode with a bioanode for glucose conversion, made of PQQ–GDH embedded into an Os-complex-modified redox polymer	Chronoamperometry/CV	N/A	Glucose/ N/A	[81]

ASV: anodic stripping voltammetric; QD: quantum dot; N/A: not available in the study; OSWV: osteryoung square-wave voltammetry; MCH: 6-mercaptohexanol; SH-NC3: mixed monolayer of thiolated DNA probe; SiNWs: silicon nanowires; CNFs: carbon nanofibers; PDA: polydopamine; PMCSPE: PBA, MWCNTs, and CS-modified screen-printed electrodes; PAH: phenylalanine hydroxylase enzyme; SH-probe: thiolated probes; *E. coli*: *Escherichia coli*; PANI: polyaniline; AuE: gold screen-printed electrodes; Cys: cysteamine; PAMAM: poliamidoamin; HIV-1, HBV, HCV, Zika, Dengue, and SARS-CoV-2: Human Immunodeficiency Virus (HIV), Hepatitis B and C Viruses, Zika Virus, Dengue Virus, and Severe Acute Respiratory Syndrome Coronavirus 2; PtNPs: platinum nanoparticles; AgNPs: silver nanoparticles; EPI: epirubicin; IDA: idarubicin; DOX: doxorubicin; ctDNA: circulating tumor DNA; MnO_2: manganese dioxide; HP-QDs-SPGE: hairpin DNA probes conjugated with water-soluble and carboxyl functionalized quaternary Zn–Ag–In–S quantum dot (QD) on SPGE; PCa: prostate cancer; PQQ: pyrroloquinoline quinone; GDH: glucose dehydrogenase; BOD: bilirubin oxidase.
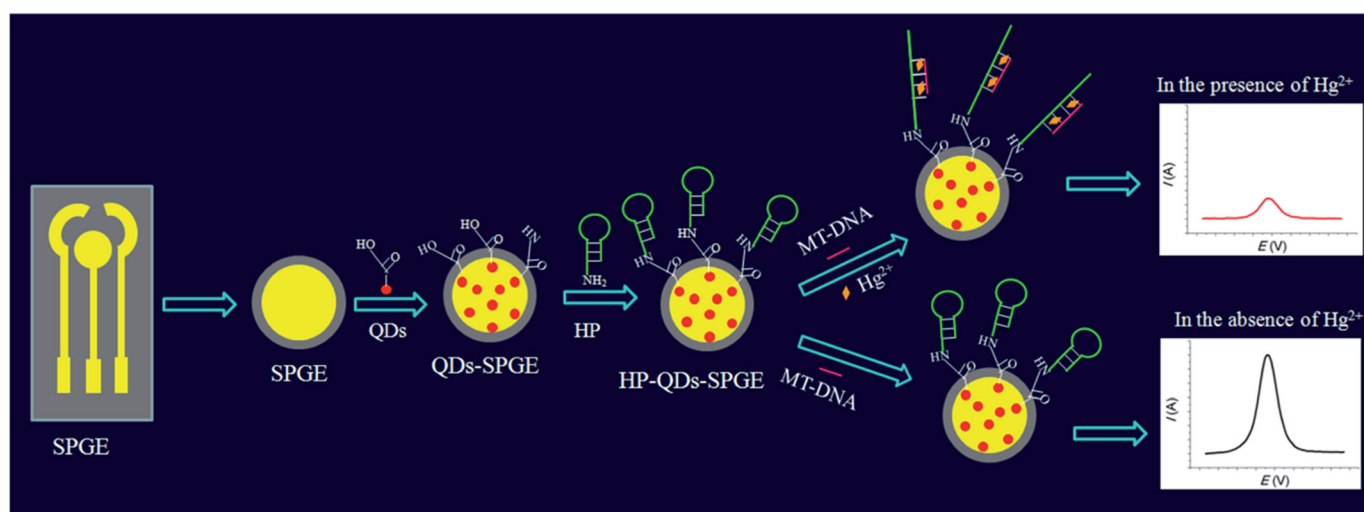

Figure 5. Schematic representation of the HP–QDs–SPGE electrochemical biosensor (adapted and reprinted with permission from [79]).

3.2. Aptasensors

Evaluating significant analytes while using electrochemical aptasensor-based sensors is important in sensor-based procedures. Of note is that the aptasensor has an enhanced affinity for diverse targets; to name a few, cells, proteins, as well as viruses could be taken into account. Indeed, small molecular substances include 15–90 oligonucleotides having short sequences of single-stranded nucleic acids (DNA or RNA) [83,84]. Since the aptamer was reported to be more sensitive in comparison with the antibodies while it reacts to minor variations through an electrochemical procedure, it is then a distinct design, especially thanks to its high selectivity [85,86]. Aptamers can be used as bio-diagnosis parts to recognize some disease mechanisms and to evaluate and detect their reasons in

addition to determining the origins. They are also of use in a wide range of scientific fields, from pharmacy to forward-thinking drug delivery systems. They are also employed in order to discover new drugs and appraise their biological activities [87]. Many examples were proposed recently for electrochemical aptamer-based sensors using SPE. Table 2 briefly presents the analytical properties and the major characteristics of some of the latest aptasensors, in addition to illustrative procedures used in biological samples [88–110]. Several chosen instances are explained below.

Although it is evident that diazinon (DZN) is one of the most extensively used organophosphorus compounds in agricultural and household applications, if its traces continue to stay in the environment, unfavorable impacts will be imposed on living creatures, including humans and animals [111,112]. Bearing this in mind, its acknowledged maximum residue limits (MRLs) were determined by health authorities, limited to 0.04 µg/kg, 0.1 µg/L, and 0.04 µg/g in soil, water, and vegetables, respectively. These determining organizations are the European Union, specifying the mentioned limit for soil and vegetables, while the Food and Agriculture Organization of the United Nations/WHO determined the limit for water [113,114]. In line with this, a highly sensitive label-free electrochemical aptasensor was devised by Hassani et al. to detect DZN. By making use of the SPGE which had been modified via thiolated aptamers being immobilized on AuNPs, it was possible to assemble the aptasensor. Nonetheless, the current selective aptasensor, which has been designed by a special method, does not present interferences from other compounds of the real samples [105].

It should be noted that breast cancer significantly leads to mortality among women and constitutes 34% of all cancer cases in women. According to scientific reports, there were more than two million new cases of this cancer in 2018 and roughly 627,000 deaths among women. Thus, it is asserted that there should be a quick diagnosis at the initial stage. Technically, tumor markers contribute considerably to quantitatively recognizing cancer. These are macromolecules in cells, blood, or other biological fluids. By considering their appearance or disparities in their concentrations, it is possible to diagnose both the appearance and the growth of the neoplastic cells. Moreover, by utilizing specific genes, it is typically possible to synthesize breast cancer biomarkers. An illustration of this is Human Epidermal Growth Factor Receptor 2 (HER2). In practice, HER2 is a gene that is accountable for HER2 protein genesis. The HER2 protein is made of three intracellular, transmembrane, and extracellular areas. These work as receptors, contributing to controlling cell growth, repair, and division to a great extent. In this context, the likelihood of survival would greatly increase once highly sensitive detection experiments are employed, ideally, employing those which will result in more rapid signals and lower expenses while being capable of offering prompt diagnoses. In line with this, an electrochemical aptasensor to detect the HER2 protein via SPGE was devised by Ferreira et al. On the one hand, the first principle was fabricated by the SAM attained from the 1-mercapto-6-hexanol (MCH) and thiolated DNA aptamers specific to the HER2 composite; on the other hand, their next principle was a ternary SAM which encompassed 1,6-hexanethiol (HDT) while having the same aptamer. Notably, these mentioned systems were additionally passivated by MCH while being blocked using bovine serum albumin (BSA). The nonspecific association to the surface of the electrode diminished significantly, as exhibited by the ternary SAM architecture, and this was attributed to the HDT antifouling characteristics [106].

Categorized as a metabolic disorder, diabetes stands as a major health issue worldwide. Issues associated with insulin supply and production in the human body are responsible for diabetes. Insulin is a hormone containing a double-chain polypeptide. To determine insulin levels, an electrochemical method was recommended by Amouzadeh's group, which is based on an aptasensor at femtomolar (fM) concentrations, in which the surface of the SPE is modified by means of the ordered mesoporous carbon, which underwent chemical modification by 1,3,6,8-pyrenetetrasulfonate (TPS) (Figure 6). In this way, with the use of the reactive sulfonyl chloride groups, the aptamer functionalized with amino groups was covalently bonded to the TPS. Afterward, the MB was intercalated with the immobilized

aptamer, which was considered in this context as the redox probe. It was possible for the modified MB to relate to the insulin, resulting in the MB release while minimizing the signal attained by the DPV [107].
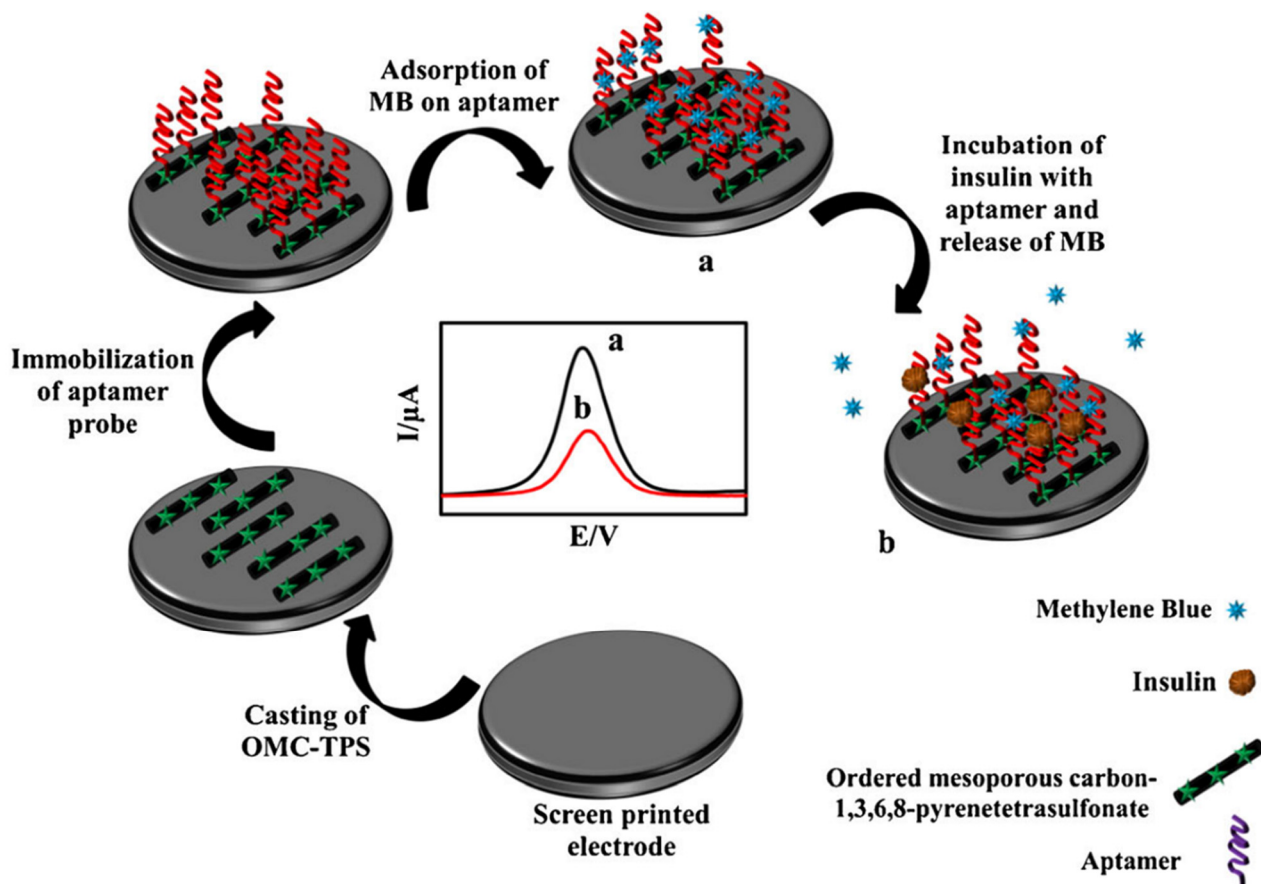

Figure 6. Schematic of aptasensor construction. Inset: responses of CSPE/OMC-TPS/aptamer-MB without insulin (**a**) and with insulin (**b**) (adapted and reprinted with permission from [107]).

Table 2. SPE aptasensors for (bio)compound detection in some samples.

Sensor Construction	Technique and Method	Detection	Analytical Characteristics	Analyte/Sample	Ref.
Apt/AuNPs/SPCE	High affinity between FB1 and its aptamer by a small association constant (Ka), calculated by the Langmuir adsorption isotherm	EIS $(Fe(CN)_6^{3-/4-})$/ CV	L.R.: 0.01–50 ng/mL LOD: 3.4 pg/mL	FB1/Corn	[88]
4-MPBA/Au NFs/SPCE	Label-free and quantitative HbA1c electrochemical bioanalysis based on the catalytic property of HbA1c	CV	L.R.: 5–1000 µg/mL LOD: N/A	HbA1c/Serum	[89]
CcR/SAM-GNP/PPy/SPCE	Covalent coupling of CcR with SAM–GNP–PPy onto the SPCE	CV	L.R.: 0.1–1600 µM LOD: 60 nM	Nitrite/Hypoxia-induced cardiac cell lines	[90]
Carbon nanomaterial (C, SWCNT, MWCNT and CNF)/SPE	Noncovalent immobilization of aptamers on the nanomaterial electrodes via π–π stacking interactions between the DNA nucleobases and the surface	SWV/CV	L.R.: 0.0001–1000 ng/mL LOD: 0.03 pg/mL	HbA1c/Human whole blood	[91]
TNT-specific peptide/SPE	A portable smartphone-based biosensing platform for TNT detection was developed with impedance monitoring on SPE	EIS $(Fe(CN)_6^{3-/4-})$	L.R.: N/A LOD: N/A	TNT/N/A	[92]

Table 2. *Cont.*

Sensor Construction	Technique and Method	Detection	Analytical Characteristics	Analyte/Sample	Ref.
CdTiPNPs-NTV/SPCE	Binding free biotin to CdTiPNPs–NTV and preventing their reaction with the sensor surface (Alb–BT)	SWASV	L.R.: 2–40 nM LOD: 1 nM	Biotin/Multivitamin tablets	[93]
Aptamer/SPE	Label-free aptasensor based on an SPE-specific adsorption to Cd^{2+} solution because of the key aptamer's high affinity for Cd^{2+}	CV/DPV	L.R.: 0.1–1000 ng/mL LOD: 0.05 ng/mL	Cadmium (II) ions/River water	[94]
MoS_2 NFs/CM/APTES/SPE	Physical and chemical reactions occurred in every step of the device surface modification to provide a higher binding affinity platform for the probe immobilization, which enhances a large number of immobilizations of biotin-linked aptamers on STVD	EIS $(Fe\,(CN)_6{}^{3-/4-})$	L.R.: 10 fM to 1 nM LOD: 10 fM	AMI biomarker (troponin I)/Human serum	[95]
Hydrazine-modified aptamer/TTCA monomer/AuNPs/SPCE	Sandwich aptamer detection was accomplished via a specific interaction between aptamers and cTnI	EIS $(Fe\,(CN)_6{}^{3-/4-})$/CV	L.R.: 1–100 pM LOD: 1 pM	cTnI/Human serum	[96]
Aptamer/AuNCs-Cys/SPGE	A label-free electrochemical aptasensor for selective CAP detection	EIS $(Fe\,(CN)_6{}^{3-/4-})$/CV/SWV	L.R.: 0.03–6.0 μM LOD: 4.0 nM	CAP/Human blood serum	[97]
Aptamer/rGO-PAMAM/Au$_{nano}$/SPE	Selective interaction of CYC with W_1/rGO-PAMAM-FAD/Au$_{nano}$/Anti-ptamer$_{CYC}$ and VEGF165 with W_2/rGO-PAMAM-Th/Au$_{nano}$/Anti-ptamerVEGF165	CV/DPV	L.R.: 2.5–320.0 pM LOD: 1.0 pM for CYC and 0.7 pM for VEGF165	CYC and VEGF165 tumor markers/Human serum	[98]
AuNPs/Fe_3O_4@SiO_2/DABCO/SPE	Label-free electrochemical aptasensor for the selective detection of epirubicin based on the specific interaction of aptamers with epirubicin and formation of the epirubicin–aptamer complex	EIS $(Fe\,(CN)_6{}^{3-/4-})$/CV/LSV	L.R.: 0.07 μM to 1.0 μM and 1.0 μM to 21.0 μM LOD: 0.04 μM	Epirubicin/Human blood serum	[99]
Zr-MOF/Fe_3O_4(TMC)/AuNCs/SPE	Antibody-labeled Zr-MOF/Fe_3O_4(TMC)/AuNCs as the signal amplification unit and rGO/APBA/SPE as the sensing platform	ECL/CV	L.R.: 2–18% LOD: 0.072%	HbA1c/Human whole blood	[100]
TBA-SWCNT/SPCE	Competitive interaction with the TBA to thrombin and SWCNT is a key role in this sensor system, which is applicable to label-free faradic impedance detection	EIS $(Fe\,(CN)_6{}^{3-/4-})$	L.R.: 0.0001–1.0 μM LOD: 0.02 nM	Thrombin	[101]
Hemin-aptamer/PEG- Au/SPE	Thrombin binding to the aptamer and formation of the DNAzyme—the G4 structure with intercalated hemin—underwent direct electron transfer (ET)	CV	L.R.: 0.5–100 fM LOD: 0.5 fM	Thrombin	[102]
Aptamer/CNFs-AuNPs/SPCE	After the incubation of SARS-CoV-2-RBD (64 nM) with the immobilized aptamer, the R_{ct} increased due to the mass transfer limiting of $Fe\,(CN)_6{}^{3-/4-}$ to the electrode surface that is caused by SARS-CoV-2-RBD (~35 kDa) as a large molecule	EIS $(Fe\,(CN)_6{}^{3-/4-})$	L.R.: 0.01–64 nM LOD: 7.0 pM	SARS-CoV-2-RBD/Human saliva samples	[103]

Table 2. *Cont.*

Sensor Construction	Technique and Method	Detection	Analytical Characteristics	Analyte/Sample	Ref.
Aptamer-SWCNT-SPEs	Binding-induced folding of the DNA aptamer in the presence of the target S1 protein leads to a concentration-dependent suppression in the registered amperometric signal	DPV	L.R.: 20−100 nM LOD: 7 nM	SARS-CoV-2 spike protein S1 subunit/Other proteins	[104]
DZN-thiolated aptamer-Au NP-SPGE	Label-free electrochemical nano-aptasensor as portable devices would be a promising approach in the fast and precise detection of DZN	EIS (Fe$(CN)_6^{3-/4-}$)/CV	L.R.: 0.1–1000 nM LOD: 0.0169 nM	Diazinon/Plasma of male Wistar rat	[105]
SAM: Aptamer + MCH-SPGEs Ternary SAM: Aptamer + HDT + MCH-SPGEs	Two different aptamer immobilization strategies (SAM and ternary SAM) were demonstrated for the detection of the HER2 protein biomarker in PBS diluted and undiluted serum using SPGEs	EIS (Fe$(CN)_6^{3-/4-}$)	L.R.:1 pg/mL–1000 ng/mL LOD: 172 pg/mL	Breast cancer (HER2)/ Human serum	[106]
Aptamer-MB/ OMC-TPS CSPE	MB as a probe can bind to the DNA chain through the preferential binding between MB and guanine bases, and the decrease in peak current intensity of the DPV of intercalated MB was monitored	EIS (Fe$(CN)_6^{3-/4-}$)/CV	L. R.:1.0 fM to 10.0 pM LOD: 0.18 fM	Insulin/Normal human serum	[107]
Cu (OH)$_2$ NRs/SPCE	In the presence of SARS-CoV-2 spike glycoprotein, a decrease in Cu(OH)$_2$ NR-associated peak current was observed that can be due to the target–aptamer complex formation and thus the blocking of the electron transfer of Cu(OH)$_2$ NRs	SWV	L. R.: 0.1 fg/mL–1.2 µg/mL LOD: 0.03 fg/mL	SARS-CoV-2/Saliva and VTM samples	[108]
Apt-AuNPs/SPE	An amperometric aptasensor with a sandwich-type architecture for the specific detection of CRP through NPs as biorecognition and signaling elements	Amperometry	L.R.: 10 pg/mL–1.0 ng/mL LOD: 3.1 pg/mL	CRP/Human serum samples	[109]
Apt/Au/SPE	Signal switch-based detection was achieved using MB-modified insulin specific aptamer	SWV	L.R.: 25–150 pM LOD: 18.5 pM	Insulin hormone/ Blood samples	[110]

FB1: fumonisin B1; CV: cyclic voltammetry; AuNPs; gold nanoparticles; HbA1c: glycated hemoglobin; N/A: not available in the study; 4-MPBA: 4-mercaptophenylboronic acid; Au NFs: gold nano-flowers; CcR: cytochrome c reductase; SAM: self-assembled monolayer; GNPs: gold nanoparticles; PPy: polypyrrole; HbA1c: glycated hemoglobin; DZN: diazinon: SPGE: screen-printed gold electrode; MCH: 1-mercapto-6-hexanol; HDT: 1,6-hexanethiol; OMC-TPS: ordered mesoporous carbon/1,3,6,8-pyrenetetra sulfonic acid; MB: methylene blue; DPV: differential pulse voltammogram; TNT: 2,4,6-trinitrotoluene; CdTiPNPs: cadmium-modified titanium phosphate nanoparticles; SWASV: square-wave anodic stripping voltammetry; CdTiPNPs: cadmium-modified titanium phosphate nanoparticles; NTV: neutravidin; SPCE: screen-printed carbon electrodes; AMI: acute myocardial infarction; MoS$_2$ NFs: 3D-flower-like MoS$_2$ nanoflowers; APTES: (3-aminopropyl) triethoxysilane; CM: complex mixture; STVD: streptavidin; cTnI: cardiac troponin I; TTCA: 5,2′:5′2″-terthiophene-3′-carboxylic acid; CAP: chloramphenicol; AuNCs: gold nanocubes; Cys: cysteine; CYC: cytochrome c; VEGF165: vascular endothelial growth factor; rGO-PAMAM/Au$_{nano}$: reduced graphene oxide/gold functionalized with poly(amidoamine) dendrimers; Fe$_3$O$_4$@SiO$_2$/DABCO: magnetic double-charged diazoniabicyclo [2.2.2] octane dichloride silica hybrid; Zr-MOF/Fe$_3$O$_4$(TMC)/AuNCs: zirconium metal-organic framework/Fe$_3$O$_4$(trimethyl chitosan)/gold nanocluster; TBA: thrombin binding aptamer; CRP: C-reactive protein; GLU: glutaraldehyde; CNFs-CHIT: carbon nanofiber–chitosan nanocomposite; Cu(OH)$_2$ NRs: copper hydroxide nanorods; VTM: viral transport medium; RBD: receptor-binding domain; CNFs: carbon nanofibers.

3.3. Immunosensors

Before discussing the components and the working principle of an immunosensor, it is necessary to clarify the immunoassay. An immunosensor refers to the mechanism where either the antibody or antibody fragments are employed as the elements to perform molec-

ular recognition for the antigens as specific analytes to create a steady complex. Yalow and Berson were the pioneering scholars introducing the immunoassay principle in 1959 [115], and they succeeded in developing the extensively employed radioimmunoassay, which was designed for assessing the attributes of insulin-binding antibodies in human serum. This was accomplished by using samples attained from patients cured with insulin. Later, a biosensor notion was presented by Clark and Lyons in 1962 for different applications [116].

The main reason these instruments were considered in food, environmental, and clinical analyses is the fact that electrochemical immunosensors incorporate specificity which is highly characteristic of the interactions between the antigen and the antibody, accomplished by higher sensitivity to electrochemical transduction. A considerable quantity of published works has elaborated on electrochemical immunosensors which have been based on the immobilization of the antibodies on an electrode surface, reacting with free antigens in the face of the labeled antigens [117]. Afterward, the interaction between them is pursued by determining the enzyme activity, including determining the specific enzyme substrate that is added. The label-free immunosensors have recently been able to detect the immune interaction between the antibody and antigen. These biosensors demonstrate some significant benefits with regard to the rate and ease of action [118].

Between these evaluations, enzyme-linked immunosorbent assay (ELISA) or enzyme immunoassay is a favored method. ELISA is extensively applied as a detection device in clinical trials. The major point in this technique is that an indistinct antigen amount is immobilized onto a surface, and then a known antibody amount is added on the surface to bind with the antigen. This antibody is linked to an enzyme, and finally, a substance is appended so that the enzyme can convert to some recognizable signal, which in a chemical substrate consistently creates optical or electrochemical variations. This method, due to its higher specificity and sensitivity in comparison with other immunoassays, is reliable [26].

SPE immunosensors are mostly engaged in on-site/point-of-care detection. SPEs are mechanically strong electrochemical converters with a low cost which allows the miniaturization of sensors and their manufacturing, which is feasible for merging the WEs and REs in the same chip. They are also single-use tools, making them beneficial in immunosensors' fabrication [119].

In this section, several examples are reported on the use of immunosensors in the analysis of different biocompounds with SPEs (Table 3) [54,120–144].

J. Fei's group offered a sandwich-type electrochemical immunoassay for *Salmonella gallinarum* and *Salmonella pullorum* based on a synthesized core shell of $Fe_3O_4/SiO_2/AuNPs$ by anchoring AuNPs on Fe_3O_4 particles with strong bonding forces between AuNPs and –SH. *S. gallinarum and S. pullorum* were used as the target bacteria. The AuNPs operated as the intermediary substances for bonding between Fe_3O_4/SiO_2-SH and the antibody and acquired the immunomagnetic nanocomposites (Ab1/AuMNPs). The HRP-labeled antibody versus *S. gallinarum* and *S. pullorum* (HRP-Ab2) was employed as the signal tag. The *S. gallinarum* and *S. pullorum* bacteria in the sample were obtained with Ab1/AuMNPs and separated from the analyte samples using an external magnetic field. The MNP–*Salmonella* complexes were redispersed in a buffer solution and then subjected to HRP-anti *S. gallinarum* and HRP-anti *S. pullorum*. The final sandwich complexes were attached on the surface of the WEs of a four-channel SPCE (4-SPCE) by an external magnetic field (Figure 7). The SPCE and 4-SPCE reproducibility were compared with CV [122].

As a growth-promoting agent, salbutamol (SAL) is a β_2-agonist that is typically utilized illegitimately in livestock. This illegitimate application could cause health risks, including cardiac palpitation, tachycardia, and muscle tremors. C.-H. Lin's group offered highly sensitive label-free impedimetric immunosensors which functioned on the basis of gold nanostructure (AuNS)-deposited SPCE. It is acknowledged that interactions of antibodies and antigens can be directly detected using label-free electrochemical immunosensors lacking fluorescence- or enzyme-labeled secondary antibodies. This eliminates the labeling and reacting methods while resulting in lower costs and time throughout the measurement procedure.

The AuNS was prepared by a two-step template and low electrodeposition in a sea urchin shape had submicrometer-scale pyramidal structures on micrometer-scale particles. AntiSAL monoclonal antibody was immobilized on the 1-ethyl-3-(3-dimethylamino-propyl) carbodiimide hydrochloride/N-hydroxysuccinimide-activated 3-mercaptoproponic acid-modified AuNS/SPCEs (Figure 8). The label-free immunosensors based on the EIS method are mostly employed in the detection of high-molecular-weight biomarkers, such as DNA and protein, but are scarcely employed to detect low-molecular-weight compounds with several hundreds of g/mol. This is because chemicals with a lower molecular weight cause fewer spatial changes in the electrochemical characteristics of the interface among the electrolyte and antibody immobilized on the electrode surface, which reduces the electrochemical signal and leads to a high LOD. Thus, conductive NSs such as AuNPs with a large surface area are significant for developing label-free EIS-based immunosensors for the detection of low-molecular-weight chemicals [127].

L. Zhao et al. offered a multiplexed, single-channel, label-free amperometric immunosensor, as shown in Figure 9, for the detection of neuron-specific enolase (NSE), squamous cell carcinoma antigen (SCCA), carbohydrate antigen 125 (CA125), and fragment antigen 21-1 (Cyfra21-1) as tumor markers. In the multiplexed SPCE immunosensor, composites of WEs on the SPCE surface were separately modified for each target, and the related signals were registered using a multi-channel electrochemical workstation [145,146]. Although these types of safety sensors have made significant progress, they have problems: (1) RE and CE contain precious metals such as Au, Pt, and g printed on single-use SPCEs, which led to increased SPCE costs and pollution with precious metals [147]; (2) due to SPCE use with multiple WEs and only one RE, the area of the RE is not much larger than that of WEs and cannot prevent the current detection interference from the CE, leading to poor immunoassay repeatability; (3) the polymeric binder presence in the carbon ink affected the SPCEs' conductivity, which seriously influenced the immunoassay sensitivity [26]; (4) a costly multi-channel electrochemical workstation is needed, resulting in a restriction of the immunoassay's vast utilization. If, by designing SPCEs with a new structure and attaching highly conductive material on WEs, these problems can be overcome, this will widely increase the possible utilizations of this immunosensor type. To improve this case, a new SPCE type with several WEs and one signal output channel but without CEs and REs was constructed. The multifold WEs are able to be separately modified for each analyte of interest, allowing the advanced SPCE to be employed in the multifold label-free immunosensor fabrication. The CEs and REs including expensive metals (Au, Ag, and Pt) were independent of single-use SPCE, which lowers the costs and eliminates the metal contamination of the SPCE. With a platinum network as CE, it was confirmed that the CE area was larger than the WE area and thus enhanced the reproducibility of the SPCE. In addition, a three-dimensional (3D) network hydrogel production method was used on the WE to increase the conductivity of the SPCE [131].

Table 3. Immunosensors for (bio) compound detection in some samples.

Sensor Construction	Technique and Method	Detection	Analytical Characteristics	Analyte/Sample	Ref.
Anti mAβ/AuNPs/DEP	Label-free impedimetric amyloid beta immunosensor on carbon DEP chip	EIS (Fe$(CN)_6^{3-/4-}$)	L.R.: 1–200 μM LOD: 0.57 nM	Amyloid beta peptide/Human serum albumin	[120]
QD-STV/ anti-H-IgA-BT/ anti-tTG IgA/SPCE	A blocking-free one-step immunosensing strategy using eight-channel screen-printed arrays for the detection of anti-transglutaminase IgA antibodies	DPV	L.R.: 3–40 U/mL LOD: 2.7 U/mL	Anti-tTG IgA antibodies/Human serum	[121]
Ag/Ab/Fe$_3$O$_4$/ SiO$_2$/AuNPs/SPCE	A sandwich electrochemical immunoassay method	CV	L.R.: 10^2–10^6 CFU/mL LOD: 32 CFU/mL	*S. pullorum* and *S. gallinarum*/Food samples (chickens)	[122]

Table 3. *Cont.*

Sensor Construction	Technique and Method	Detection	Analytical Characteristics	Analyte/Sample	Ref.
Anti-HSA/ EDC + NHS/ COOH-P-SPCE	A simple and sensitive electrochemical immunosensor based on carboxyl-enriched porous SPCE for detecting urinary albumin in the range of microalbuminuria	CV/CA	L.R.: 10–300 µg/mL LOD: 9.7 µg/mL	Microalbuminuria/ Urine	[123]
BSA/HRP/Ab2/ CEA/Ab1/EDC + NHS/AuNPs/ rGO/SPEs	A sandwich type immunosensor to mimic the ELISA (enzyme-linked immunosorbent assay) immunoassay	CV	L.R.: 0.5–2000 ng/mL LOD: 0.28 ng/mL	CEA/N/A	[124]
PPY/CEA/Ag-SPE	Combination of the novel PCB-based SPEs comprising Ag tracks with the use of an antibody-like biomimetic material as a sensing element	CV/SWV/ EIS $(Fe\,(CN)_6^{3-/4-})$	L.R.: 0.05–1.25 pg/mL LOD: N/A	CEA/Urine	[125]
Ab/fG/SPE	A convenient graphene SPE platform for nonenzymatic label-free immunosensors	EIS $(Fe\,(CN)_6^{3-/4-})$	L.R.: 0.1–1000 ng/L LOD: 52 pg/L	Parathion/Tomato and carrot	[126]
Antibody SAL/EDC + NHS-activated MPA/AuNS/SPCEs	The high roughness and conductivity of AuNS allowed the immunosensor to have more immobilized antibodies and a smaller interface impedance, resulting in a lower LOD than the one using flat AuDEs	EIS $(Fe\,(CN)_6^{3-/4-})$	L.R.: 0.1 pg/mL–1 µg/mL LOD: 4 fg/mL	SAL/Serum samples	[127]
Ab/rGO-TEPA/AuNPs/SPE	A disposable sandwich immunosensor for sensitive electrochemical detection of AFP through the combination of SPEs and paper-based microfluidic channels	SWV	L.R.: 0.01–100 ng/mL LOD: 0.005 ng/mL	AFP/Serum samples	[54]
Ab/AgNPs-rGO/SPE	The sandwich-type immunosensor, which yielded a lower LOD than its nonsandwich counterpart	CV	L.R.: 0.05–0.40 µg/mL LOD: 0.042 µg/mL	CEA/N/A	[128]
HER2 Ag/Ab/SPE	Unmodified SPEs fabricated for HER2 detection antigen using the traditional sandwich ELISA protocol without compromising on the accuracy, precision, or sensitivity of the device	CV	L.R.: 5–20 ng/mL and 20–200 ng/mL LOD: 4 ng/mL and 5 ng/mL	HER2/Serum samples of invasive and non invasive breast cancer patients	[129]
AQ-2°Ab/ Anti-1°Ab/ L-Cys/Au/SPGE	A dual-working electrode was custom-designed to simultaneously compare the presence and absence of CRP to reduce the analysis time	DPV	L.R.: 0.01–150 µg/mL LOD: 1.5 ng/mL	CRP/Serum samples	[130]
(1) Ab/PoPD-Au/ Pd-SA-AuNP/SPE (2) Ab/PMB-Au/ Pd-SA-AuNP/SPE (3) Ab/PPPD-Au/ Pd-SA-AuNP/SPE (4) Ab/PTMB-Au/Pd-SA AuNP/SPCE	Multiplexed label-free immunosensor, where one signal output channel could make the immunosensor be realized by a common single-channel electrochemical workstation	SWV	L.R.: 0.01–100 ng/mL for SCCA 0.01–100 ng/mL for Cyfra21-1 0.01–200 U/mL for CA125 0.01–200 ng/mL for NSE LOD: 5.5 pg/mL for SCCA 4.8 pg/mL for Cyfra21-1 0.0054 U/mL for CA125 2.3 pg/mL for NSE	SCCA, Cyfra21-1, CA125, NSE/Serum samples	[131]

Table 3. *Cont.*

Sensor Construction	Technique and Method	Detection	Analytical Characteristics	Analyte/Sample	Ref.
(1) HC/BSA/ PRF+1/SPCE (2) JIA/BSA/ PRF+1/SPCE	The PRF+1 mimetic peptide used as a recognition biological element was successfully immobilized onto the SPCE surface, and a 15-fold increase in the current intensity was observed when compared to the bare electrode	DPV/ EIS (Fe $(CN)_6^{3-/4-}$)	N/A	JIA/Serum samples	[132]
(1) Ab_{EGFR} Cd(II)@LP/MIP/ DSP-SPE (2) Ab_{VEGF}-Cu(II) @LP/MIP/DSP-SPE	Development of electrochemical biosensors based on both MIP and antibodies for sandwich assays in the dual detection of EGFR and VEGF	EIS (Fe $(CN)_6^{3-/4-}$)	L.R.: 0.05–50,000 pg/mL for EGFR 0.01–7000 pg/mL for VEGF LOD: 0.01 pg/mL for EGFR 0.005 pg/mL for VEGF	EGFR and VEGF	[133]
BSA/Ab2/NR- Au@Pt/rGO/*E.coli* O157:H7/BSA/Ab1/ AuNPs/PANI/SPCE	The anti *E. coli* O157:H7 monoclonal antibody (Ab1) was automatically adsorbed on the AuNPs/PANI/SPCE platform through amino and AuNPs interaction. NR-Au@Pt/rGO as the nonenzyme signal label can enhance the performance of the immunoassay for the catalytic reduction of H_2O_2	CV	L.R.: 8.9×10^3–8.9×10^9 CFU/mL LOD: 2.84×10^3 CFU/mL	*E. coli* O157:H7/Pork samples	[134]
Pt/rGO/ P3ABA/SPCE	The biocompatible P3ABA contains an abundance of carboxylic groups, used as the matrix for the immobilization of enzymes (GOx or ChOx) via amide linkages to increase enzyme loading, to enhance the sensitivity and specificity, and to improve the stability of the modified electrode	CV/ EIS (Fe $(CN)_6^{3-/4-}$)/ Amperometry	L.R.: 0.25–6.00 mM for glucose 0.25–4.00 mM for cholesterol LOD: 44.3 µM for glucose 40.5 µM for cholesterol	Glucose and cholesterol/Serum samples	[135]
Au-Mab-hCG/ hCG/Mab-FSH/ SWCNTs/SPCE	A sandwich-type immunoassay, where the gold-linked second antibody (Au-Mab-hCG) was used as a label and the signal amplification strategy-using AuNPs as bio-trackers and SWCNT enhanced electron transfer nearly double that of bare SPCE	DPV	L.R.: 10–1000 pg/L LOD: 5 pg/L	hCG/N/A	[136]
PSA/anti-PSA/ GO/SPCE	The sensing platform comprises a direct-type immunoassay which involves the selective interaction of PSA with anti-PSA	CV/ EIS (Fe $(CN)_6^{3-/4-}$)	L.R.: 0.75–100 ng/mL LOD: 0.27 ng/mL	PSA/Human (male) blood serum sample	[137]
Ag/Ab/15 nm AuNPs-SPE	The surface modification of carbon SPEs with AuNPs could increase the electron transfer rate between the electrolytic solution and the modified electrode compared with that of bare SPE	CV/DPV/ EIS (Fe $(CN)_6^{3-/4-}$)	L.R.: 10–10^6 CFU/mL LOD: 13 CFU/ml	MRSA/Pathogenic bacteria	[138]
MBs/ anti-rabbit IgG-AP/ anti-SARS-CoV antibody/CB/SPE	The electrochemical assay was conceived for spike (S) protein or nucleocapsid (N) protein detection using magnetic beads as the support of the immunological chain and the secondary antibody with alkaline phosphatase as the immunological label	DPV	L.R.: N/A LOD: 19 ng/mL in buffer solution and 8 ng/mL in untreated saliva	SARS-CoV-2/Saliva and nasopharyngeal swab samples	[139]

Table 3. *Cont.*

Sensor Construction	Technique and Method	Detection	Analytical Characteristics	Analyte/Sample	Ref.
AuDdrites/SPCE	A flexible and label-free immunosensor chip made with tree-like gold dendrites (AuDdrites) was electrochemically formed by selective desorption of l-cysteine (L-cys) on (111) gold planes	SWV	L.R.: 0.1–900 ng/mL LOD: 0.03 ng/mL	25(OH)D3/Serum samples	[140]
GFAP/BSA/ GFAP Ab/ Au@ZIF-8@rGO/SPE	The concept of the immunosensor is to detect the signal perturbation obtained by measuring the changes in the load transfer resistance of the electrode by using $Fe(CN)_6^{3-/4-}$ measurements after binding the protein during incubation	CV/ EIS ($Fe(CN)_6^{3-/4-}$)	L.R.: 50–10,000 fg/mL LOD: 50 fg/mL	GFAP/Urine samples	[141]
AFB1-mAb/MB-OVA-AFB1/CB/SPE	A user-friendly smartphone-based magneto-immunosensor on CB/SPE modified electrodes for point-of-care detection of aflatoxin B1	CV/EIS ($Fe(CN)_6^{3-/4-}$)	L.R.: N/A LOD: 13 pg/mL in buffer solutions and 24 pg/mL in corn samples	Aflatoxin B1/Corn samples	[142]
S1-IgG antibody and S1 protein/ AuNP/SPE	A one-step and specific detection of SARS-CoV-2 virus from unprocessed clinical samples	SWV	L.R.: 0.1 fg/mL–100 pg/mL LOD: 7.62 fg/mL	SARS-CoV-2/Swab and blood samples	[143]
AbD/CYM/ Au@MNPs/SPE	Modifications were set up to maximize the diffusion of the probe on the electrode surface, therefore amplifying the current decrease occurring after the 25(OH)D$_3$ interaction due to both the steric hindrance and the lipophilic nature of molecule	DPV	L.R.: 7.4–70 ng/mL LOD: 2.4 ng/mL	Vitamin D$_3$ (25-OHD$_3$)/ Untreated serum samples	[144]

DEP: disposable electrochemical printed; Anti mAβ/: N-terminal human monoclonal Aβ antibody; tTG: anti-tissue transglutaminase antibodies; QD-STV: Qdot-streptavidin conjugate; *S. pullorum*: *Salmonella pullorum*; *S. gallinarum*: *Salmonella gallinarum*; CA: chronoamperometric; HAS: human serum albumin; COOH-P-SPCE: carboxyl porous screen-printed carbon electrode; AuNPs/rGO: gold nanoparticles and reduced graphene oxide; CEA: carcinogenic embryonic antigen; N/A: not available in the study; fG: functionalized graphene; SAL: salbutamol; MPS: 2-(N-morpholino) ethanesulfonic acid; rGO-TEPA: reduced graphene oxide-tetraethylene pen-tamine; AFP: alpha-fetoprotein; AgNPs: silver nanoparticles; HER2: Human Epidermal Growth Factor Receptor-2; CRP: C-reactive protein; L-Cys: L-cysteine; Anti-1°Ab: unlabeled capture primary antibody; AQ-2°Ab: anthraquinone-labeled signaling secondary; SCCA: squamous cell carcinoma antigen; Cyfra21-1: fragment antigen 21-1; CA125: carbohydrate antigen 125; NSE: neuron-specific enolase; JIA: juvenile idiopathic arthritis; HC: healthy control; PRF+1: PRF+1 mimetic peptide; EGFR: epidermal growth factor receptor; VEGF: vascular endothelial growth factor; MIP: molecularly imprinted polymer; LP: liposomal; DSP: 3,3′-dithiodipropionic acid di(N-hydroxysuccinimide ester); *E. coli* O157:H7: *Escherichia coli* O157:H7; Au@Pt: Gold@platinum nanoparticles; PANI: polyaniline; NR: neutral red; P3ABA: poly(3-aminobenzoic acid); hCG: human chorionic gonadotropin; Mab: monoclonal anti-human α-subunit; FSH: follicle-stimulating hormone; PSA: prostate-specific antigen; MRSA: Methicillin-resistant *Staphylococcus aureus*; OA: okadaic acid; FL-WO3: flower-like WO$_3$-modified screen-printed electrode; MBs: magnetic beads; CB: carbon black; 25(OH)D3: 25-hydroxyvitamin D3; GFAP: glial fibrillary acidic protein; Au@ZIF-8@rGO: zeolitic imidazolate frameworks and reduced graphene oxide anchored with gold nanoparticles; CB: carbon black; AFB1-mAb: monoclonal antibody specific for aflatoxin B1; MB-OVA-AFB1: magnetic beads conjugated with AFB1-OVA; CYM: cysteamine hydrochloride; Au@MNPs(AuMNPs): core–shell magnetic nanoparticles (Au-covered iron oxide nanoparticles); AbD: vitamin D3 antibody.
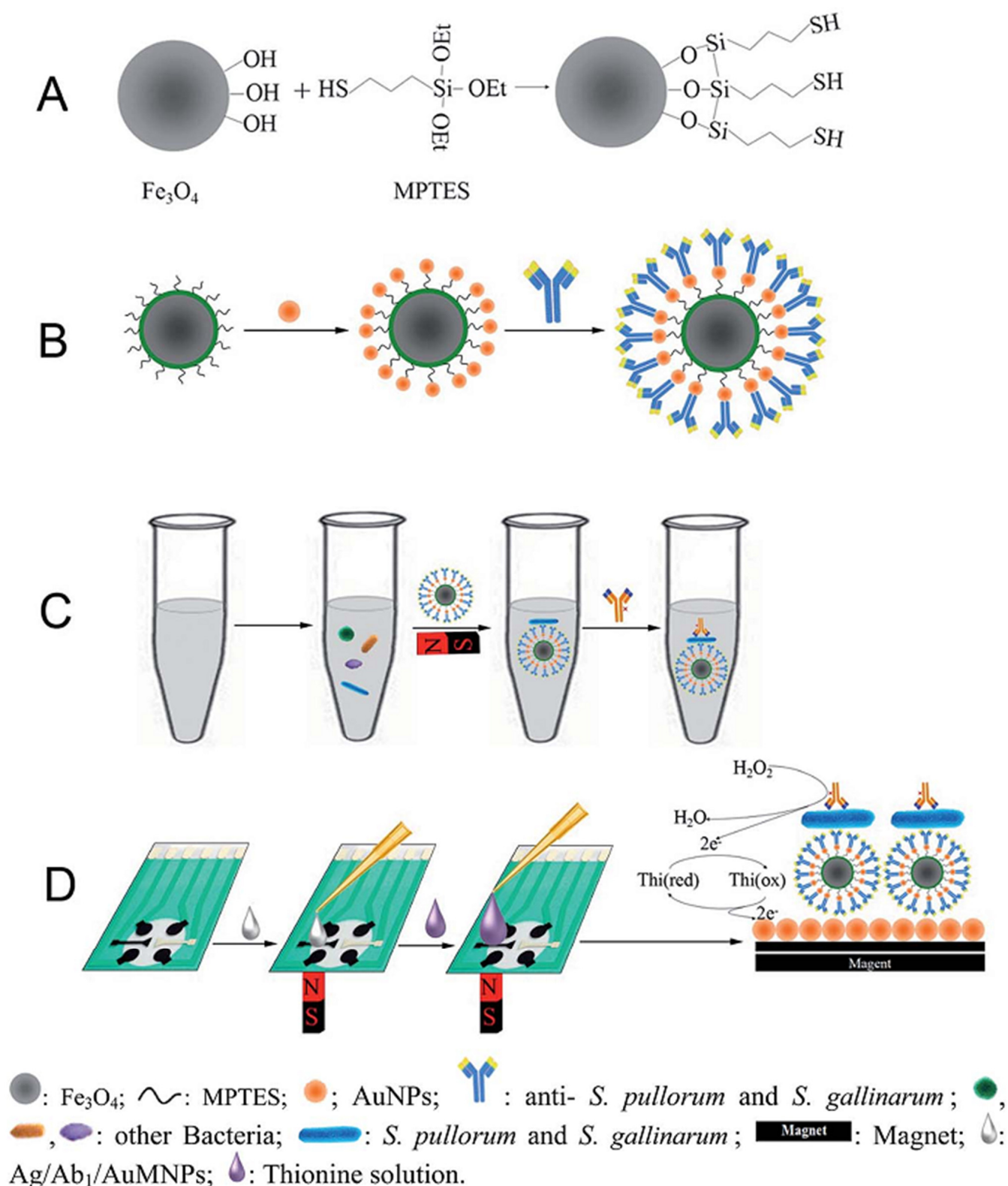
Figure 7. Schematic of the modification process of the electrochemical immunoassay and the detection mechanism: (**A**) the synthesis process of the Fe$_3$O$_4$/SiO$_2$–SH nanoparticles; (**B**) the synthesis process of Ab$_1$/AuMNPs; (**C**) the process of *S. pullorum* and *S. gallinarum* being captured from the samples by Ab$_1$/AuMNPs and the formation of HRP-Ab$_2$/Ag/Ab$_1$/AuMNPs; (**D**) HRP-Ab$_2$/Ag/Ab$_1$/AuMNPs dropped on AuNPs/4-SPCE, which is the principle of electrochemical detection (adapted and reprinted with permission from [122]).
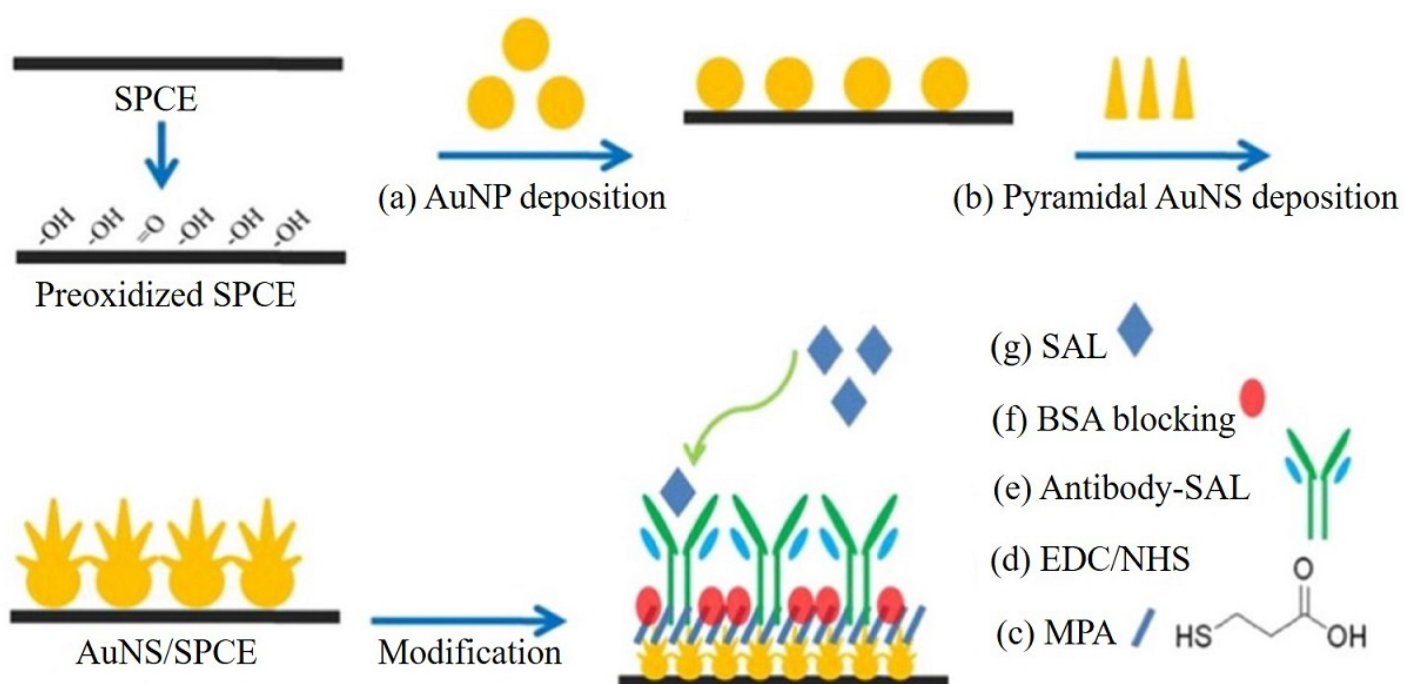
Figure 8. Schematic processes of the immunosensor construction (adapted and reprinted with permission from [127]).
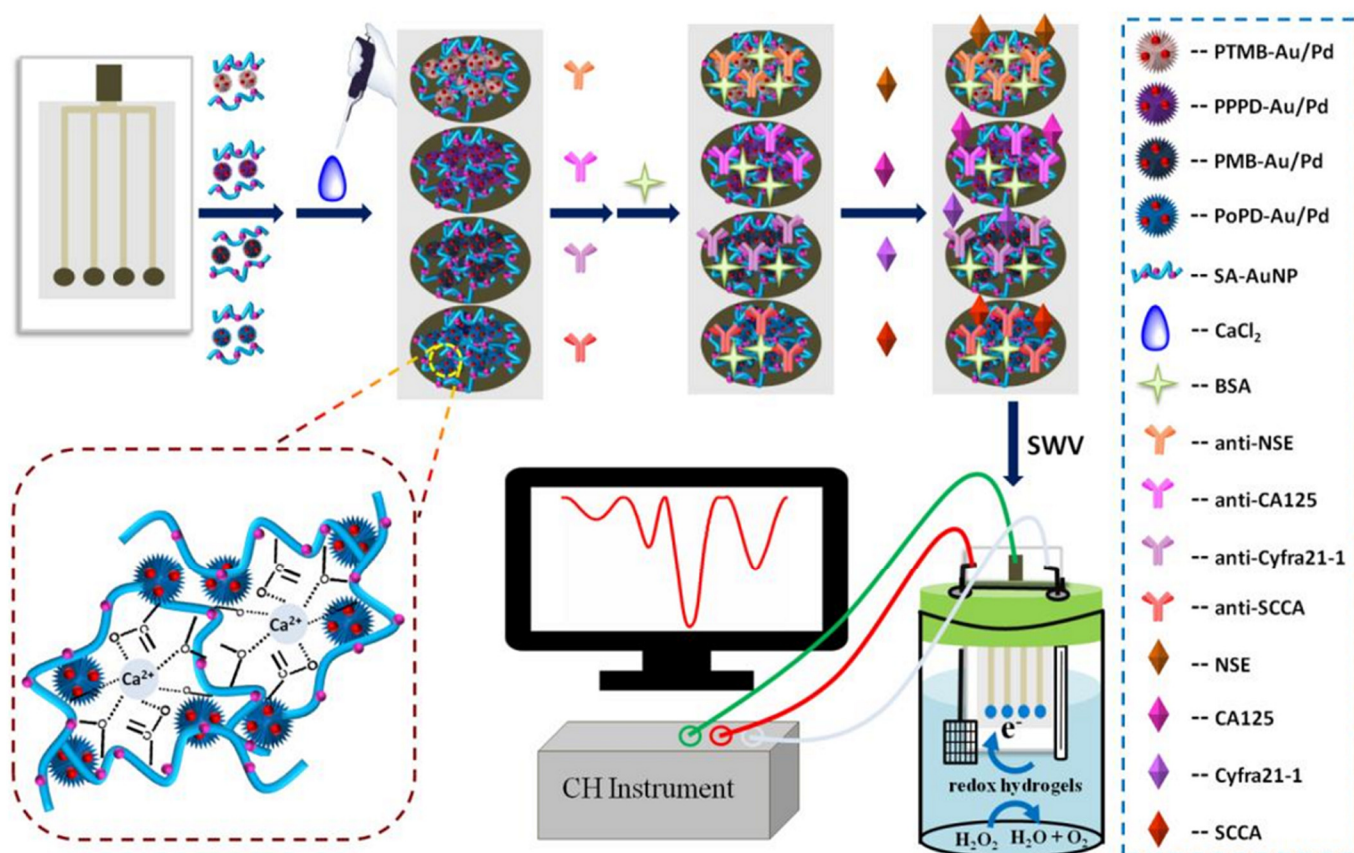
Figure 9. Schematic illustration of the offered label-free amperometric immunosensor by using the modified SPCE (adapted and reprinted with permission from [131]).

3.4. Enzyme Biosensors

Although there are higher expenses involved in extracting, isolating, and purifying enzymes, they are repeatedly utilized as biological substances to fabricate biosensors. This is because of their fast and clean formation of selective bonds with the substrate. As proteins with polypeptide structures, enzymes catalyze certain chemical reactions in vivo, accelerating the reaction rate. While enzymes were reported to be the first employed in biosensors, they are currently being used widely and extensively. In fact, their specificity has been considered as their main favorable characteristic, enabling their use in biosensor methods. Contrary to chemical catalysts, enzymes yield significantly higher levels of substrate specificity. This occurs due to the restrictions forced onto the substrate molecule by the active site environment, which encompasses factors such as functional groups, stereochemistry, molecular size, polarity, and relative bond energies [1]. The operation of the enzyme biosensors consists of the most selective interaction between the target analyte and the active sites of the enzyme. This results in the formation of a complex that is capable of converting the analyte into one or more products. By appraising the quantity of the obtained product, the analyte could be thus detected. Nevertheless, there is occasionally a need for cofactors or coreagents, which is why they could be likewise used with the aim of presenting the interaction between the enzyme and the analyte [29,148].

G. Hughes et al. scrutinized an SPCE encompassing the electrocatalyst Meldola blue (MB) as the base transducer for a reagentless glutamate biosensor. This was accomplished as the components were deposited sequentially through a layer-by-layer procedure. As such, for encapsulating the enzyme glutamate dehydrogenase (GLDH) and the cofactor nicotinamide adenine dinucleotide (NAD^+), the researchers made use of MWCNTs and biopolymer chitosan (CHIT). Poor homogenous dispersion resulted from the slight solubility of the unmodified MWCNTs. Therefore, they were suspended in a solution enclosing CHIT, which is considered to be a natural polysaccharide. This practice originated from crustaceans, revealing brilliant and striking film-forming characteristics, which enhance enzyme stability [149,150]. In opposition to other solvents, MWCNTs' dispersion in CHIT/HCl yielded the smallest particle size, forming a larger surface area while requiring no functionalization. Such a reagentless device made via the mentioned procedure is advantageous, yielding cost-efficient biosensors. Such biosensors are claimed to be convenient to use because of the fact that there is no need for any additional cofactors to be added to the sample solution [151].

Table 4 briefs the analytical features and the significant characteristics of some of the recent enzyme biosensor-based SPEs which employed the illustrative procedures in biological samples [151–180]. Some examples of these papers are explained below.

The presence of pathogenic bacteria in foods has consistently posed a serious threat to people's health and the income of food producers. Therefore, it is of great importance to use advanced recognition procedures that can identify these pathogens with high sensitivity and speed. *Escherichia coli* (*E. coli*) O157:H7 is the most common Shiga toxin-producing variant of *E. coli* in North America that can cause disease with a very low dose: between 10 and 100 cells. The symptoms of this disease consist of bloody diarrhea, intense stomach cramps, vomiting, or even the life-threatening hemolytic uremic syndrome. M. Xu's group reported an electrochemical biosensor for the fast recognition of *E. coli* O157:H7 using screen-printed interdigitated microelectrodes (SP-IDMEs) which were modified by the combination of bi-functional polydopamine-glucose oxidase (PDA-GOx)-based polymeric nanocomposites (PMNCs) and Prussian blue (PB). First, along with the selfpolymerization of DA (dopamine), the core shell magnetic beads (MBs)-GOx@PDA PMNCs were synthesized. Then, the dispersion of AuNPs was accomplished by biochemical synthesis on the surface of PMNCs to gain greater high-performance adsorption of GOx and antibodies (ABs). The ABs/GOx$_{ext}$/AuNPs/MBs–GOx@PDA PMNCs, as the final product (Figure 10), acted as the carrier to separate target bacteria from food matrices and also as the booster and modifier of the SPE in order to run electrochemical evaluations (Figure 11). The separation of unbending PMNCs was performed using a filtration process, and then, in order to

enable the occurrence of the enzymatic reaction, it was transferred into a glucose solution. The process of filtration assistance was conducted in isolation and with a concentration of free PMNCs; however, the elimination of the bonded PMNCs caused a reduction in the background noise during detection so that the sensitivity of the developed biosensor could be proportionally enhanced [152].

M. Asim Akhtar et al. reported an electrochemical biosensor to glucose analysis with functionalized graphene (f-Gr) that was assembled on the surface of a gold-sputtered SPE. Sputtering of the conducting substances such as gold and carbon on the WE present benefits in increasing the electron transfer and giving a vast spectrum of active sites for extra modifications. In addition, the dispersed AuNPs produced such an environment that the biological activity of biomolecules was maintained during immobilization while it was possible to accelerate the electron transfer between biomolecules and electrode surfaces. The thiolation of hydroxyl and epoxide groups in graphene oxide (GO) was realized by one-pot monothiolation, which was accomplished by hydrobromic acid to reduce GO, followed by the addition of thiourea and hydrolysis by sodium hydroxide to create GO-SH. Owing to the regeneration of the sp^2 carbon network and the lower electronegativity of sulfur, the electrical conductivity was increased. During immobilization of 1-ethyl-3-(3-(dimethylamino) propyl) carbodiimide, the carboxylic groups of the Gr backbone increased, which presented further active sites for the distant functional groups in GOx. The increase in the electrochemical performance may be due to the bifunctionality of the Gr backbone and the Au-sputtered morphology. AuNPs were deposited on the SPE interface that imprinted nano-island-like Au structures on the underlying carbon layers. Eventually, Gr functionalized with thiol groups was used in the modification of Au-sputtered SPE for glucose analysis (Figure 12) [153].

In order to design a reagent-free electrochemical NAD^+-dependent dehydrogenase, J. Pilas et al. presented a facile approach for the modification of SPCE with GO (Figure 13). By modifying the SPEs with the GO in addition to an additional layer of the cellulose acetate, enzymes and cofactors ((NAD^+) and $Fe(CN)_6^{3-}$) were immobilized. Notably, NAD^+ has a pivotal role as an oxidizing agent in numerous central metabolic pathways. As such, the cofactor is responsible for the electron transfer of the dehydrogenase-catalyzed reactions. Hence, the mentioned enzymes have recently attracted attention when designing electrochemical biosensors, and the reason is that there is a high degree of availability for NAD^+-dependent dehydrogenases for diverse analytes.

Generally, research in the construction of reagent-free systems focuses mostly on the advancement of biosensors for single-analyte detection. For environmental, pharmaceutical, and clinical samples, there is greater interest in more simultaneous metabolite detection. In this view, the use of an electrode array for several analytes seems important. Therefore, in this work, a multianalyte biosensor array for simultaneous and crosstalk-free determination of the metabolites L-lactate, D-lactate, ethanol, and formate was evaluated [154].

Table 4. Enzymatic biosensors for (bio)compound detection in some samples.

Sensor Construction	Technique and Method	Detection	Analytical Characteristics	Analyte/Sample	Ref.
ChOx/SiO$_2$/AuSPE	ChOx/SiO$_2$ exhibits the characteristics of the typical Michaelis–Menten kinetic mechanism with the signal saturation upon the addition of high choline concentrations	CV/Amperometry	L.R.: 0.02–0.6 mM LOD: 6 μM	Choline/Baby food samples	[155]
MWCNT-CHIT-MB/ GLDH-NAD$^+$-CHIT/ MWCNT-CHIT/ SPCE	A reagentless amperometric glutamate biosensor based on GLDH and NAD$^+$ integrated with a disposable SPE	Amperometry	L.R.: 7.5–105 μM LOD: 3 μM	Glutamate/Food, serum and clinical samples	[151]

Table 4. *Cont.*

Sensor Construction	Technique and Method	Detection	Analytical Characteristics	Analyte/Sample	Ref.
BSA-glutaraldehyde-uricase/PPD/SPE	The uricase as an enzyme on an SPE has been integrated onto a mouthguard platform along with anatomically miniaturized instrumentation electronics featuring a potentiostat, microcontroller, and a BLE transceiver	Amperometry	L.R.: 100–250 μM LOD: 2.32 μM	SUA/Human saliva samples	[156]
Ty-SWCNT-COOH/SPE	The -COOH functionalized SWCNT provides a suitable microenvironment for the immobilization of enzymes retaining the bioactivity of Ty	Amperometry	L.R.: 5–180 μM LOD: 0.62 μM	Tyramine/Pickled and smoked fish samples	[157]
GOx/4-APBA/SPCE	Glucose reacts with oxygen to generate hydrogen peroxide and gluconic acid	CV/Amperometry	L.R.: 0.05–100 mM LOD: 0.86 μM	Glucose/Blood serum, soft drink, sweet tea, and apple juice samples	[158]
ABs/GOxext/AuNPs/MBs-GOx@PDA PMNCs/SPE	The bifunctional PMNCs contain a high load of enzyme and can optimally utilize the binding sites on bacterial cells, which efficiently amplify the signal	CV/Amperometry	L.R.: 10^3–10^6 cfu/g LOD: 190 cfu/g	*E. coli* O157:H7/Foodborne pathogens	[152]
GA/ADH/PNR/AuNPs/MWCNTs/SPCE	Investigation of changes in conductivity and the electrocatalytic activity of the electrodes upon modifications	Amperometry	L.R.: 320.2–1000 μM LOD: 96.1 μM	Ethanol/Commercial alcoholic beverages	[159]
MWCNT/FcMe/CS/HRP/BSA/LOx/SPBGE	Potentially utilized as a nonintrusive point of care sensor	Amperometry	L.R.: 30.4–243.9 μM LOD: 22.6 μM	L-lactate/Embryonic cell culture	[160]
AChE/MWCNTs/DCHP/SPE	The CV responses were associated with the inhibition of AChE activity based on the amount of the added pesticide	CV	L.R.: 0.05–10^5 μM LOD: 0.05 μM	Chlorpyrifos/Vegetable samples.	[161]
ε-FK/FAOx/Ru-complex/SPE	A disposable electrochemical enzyme sensor strip for the measurement of GA using FAOx, and hexaammineruthenium (III) chloride (Ru complex) as the electron mediator	Amperometry	L.R.: 0.05–10^5 μM LOD: 0.05 μM	GA/Albumin	[162]
GOx/PBNCs/AgNWs/SPE	The combination of high electrocatalysis of PBNCs and fast conductivity of AgNWs to exhibit the synergic effects in the electrocatalytic detections	Amperometry	L.R.: 0.01–1.3 mM LOD: 5 μM	Glucose/Blood serum sample	[163]
ChOx/NiO/SPE-Au	This electrode was assembled with ChOx to develop a first-generation cholesterol biosensor where the enzymatically generated H_2O_2 was used to sense the cholesterol concentration	CV/Amperometry	L.R.: 0.067–0.6 mM LOD: 20 μM	Cholesterol/N/A	[164]
ADH/RuO$_2$-GNR/SPCE	This approach allowed increased communication and electron transfer between the electrode surface and redox centers in the ADH	CV/EIS/Amperometry	L.R.: 1–1800 μM for ethanol 1 to 1300 μM for NADH LOD: 0.19 μM for ethanol 0.52 μM for NADH	Ethanol and NADH/Commercial alcoholic beverages	[165]
GA/ADH/AuNPs/PNR/MWCNTs/SPCE for ADH and GA/G/AOx/AuNPs/PNR/MWCNTs/SPCE for AOx	The first biosensor based on ADH responds only to ethanol, whereas the second biosensor based on AOx responds to both methanol and ethanol	CV	L.R.: 178.5–1000 μM for ethanol 335.9–1000 μM for methanol LOD: 53.5 μM for ethanol 100.8 μM for methanol	Ethanol, methanol and their mixtures/Commercial alcoholic drink	[166]

Table 4. *Cont.*

Sensor Construction	Technique and Method	Detection	Analytical Characteristics	Analyte/Sample	Ref.
LOx–Cu-MOF/ CS/Pt/SPCE	A LOx-based biosensor to determine lactate in a wide concentration range	Amperometry	L.R.: 0.75 µM–1 mM LOD: 0.75 µM	Lactate/Sweat and saliva	[167]
Tyr/AuNPs/SPCE	Catechol, phenol, caffeic acid, and tyrosol were analyzed individually, and adequate analytical and kinetic performances were obtained	Amperometry	L.R.: 2.5–20 µM LOD: 0.4 nM for catechol and 0.5 µM for phenol	Total phenolic content/Commercial beers	[168]
ADH/RA/SPCE	RA/SPCE was found to facilitate the electrocatalytic oxidation of NADH by the action of RA as a natural antioxidant mediator	CV/Amperometry	L.R.: 23.71–1000 µM LOD: 7.1 µM	Ethanol and NADH/Commercial alcoholic drink	[169]
GOx/GO-SH/ Au/SPE	The enhanced electrochemical performance is originated from sputtered morphology of Au and the bifunctionality of the graphene backbone	CV	L.R.: 3–9 mM LOD: 0.3194 mM	Glucose/Various biomolecules such as cholesterol and D-alanine	[153]
PDA@ChOx/ MWCNTox/ PB/SPE	Combination of electrocatalytic properties of surfactant-modified PB films and the large high surface-to-volume ratio of CNTs	CV/EIS/Amperometry	L.R.: 0–400 µM LOD: 11 µM	Cholesterol/Biological matrices	[170]
GOx/AuNP/PANI/ rGO/NH$_2$-MWCNTs/ SPCE	The electrochemical analysis has been followed at different stages of glucose oxidase coating on modified SPCE using cyclic voltammetry	Amperometry	L.R.: 1–10 mM LOD: 64 µM	Glucose/Human blood serum samples	[171]
GOx/SiO$_2$-ATO/ PB/SPE	The used PB pigment is prepared by chemically growing a thin PB layer on the surface of SiO$_2$ particles covered by the thin shell of ATO, which was combined with a Viton® binder system	Amperometry	L.R.: 0.1–1mM LOD: 54.1 µM	Glucose/ N/A	[172]
GGP/GA/ ZnONPs/PtSPE	The PtSPE was modified with less than 5 nm ZnONPs and glutaraldehyde as a linker agent; GGPs as a biological recognition element exhibited sufficient catalytic activity towards H$_2$O$_2$ reduction	CV/Amperometry	L.R.: N/A LOD: 84 µM	H$_2$O$_2$/ N/A	[173]
(1) DAOx/PVF/ GRO/SPCE (2) MAOx/PVF/ GRO/SPCE	MAOx/PVF/GRO/SPCE showed higher sensitivity for tyramine determination in comparison with the DAOx/PVF/GRO/SPCE	CV	L.R.: 0.99–120 µM for DAOx 0.99–110 µM for MAOx LOD: 0.41 µM for DAOx 0.61 µM for MAOx	Tyramine/Cheese sample	[174]
CB/PBNPs/SPE	The versatile analysis of different pesticides was carried out by folding and unfolding the filter paper-based structure, without adding any reagents and multiple sample treatment	Amperometry	L.R.: 2–100 ppb for paraoxon 100 and 1000 ppb for 2,4-dichlorophenoxyacetic acid 10 and 100 ppb for atrazine LOD: 2 ppb for paraoxon 50 ppb for 2,4-dichlorophenoxyacetic acid for atrazine 5 ppb for atrazine	Pesticides (paraoxon, 2,4-dichlorophenoxyacetic acid, and atrazine)/ Water sample	[175]
CA/Enzymes/ GO+cofactors/SPE	NAD$^+$ and Fe(CN)$_6^{3-}$ as cofactors for ADH, DIA, FDH, DLDH, and L-lactate dehydrogenase (L-LDH) enzymes	Amperometry	L.R.: 0.25–4 mM for L-lactate, D-lactate and formate 0.05–2 mm for ethanol LOD: N/A	L-lactate, D-lactate, ethanol and formate	[154]
Uricase/Chi-Gr cry/PB/SPCE	Amperometric detection of UA catalyzed by uricase was based on the change in the cathodic current of PB at a potential of 0.00 V in a flow injection system	CV/Amperometry	L.R.: 0.0025–0.40 mM LOD: 2.5 µM	UA/Human serum samples	[176]

Table 4. *Cont.*

Sensor Construction	Technique and Method	Detection	Analytical Characteristics	Analyte/Sample	Ref.
e-Lac/CB/SPE	ESD process was exploited for the immobilization of laccase enzyme on CB/SPE	CV/Amperometry	L.R.: 2.5–50 µM LOD: 2.0 µM	Phenolic compound/ drinking, surface, and wastewater	[177]
LOx/PBNcs/SPE-BC	Handmade SPE was prepared on oxidized BC substrate and was modified with PBNcs as an electrochemical mediator to facilitate the electron transfer capability and enhance the biosensor sensitivity	CV/Amperometry	L.R.: 1–24 mM LOD: 1.31 mM	Lactate/ artificial sweat	[178]
LOx/GMgOC/SPE	The lactate sensing system features an integrated microfluidic sweat collector fabricated from polydimethylsiloxane	CV/Amperometry	L.R.: 0.1–100 mM LOD: 0.3 mM	Lactate/Sweat	[179]
E/NPs/SPCEs	Acetylthiocholine iodide, serotonin, and β-D-phenolphthalein glucuronide as E gold nanoparticles and carbon nanotubes as NPs	Amperometry	L.R.: 0.18–1.60 µg/L for AB Fubinaca 0.18–2.00 µg/L for AB Pinaca LOD: (0.07–0.10) µg/L for AB Fubinaca (0.08–0.09) µg/L for AB Pinaca	AB-Fubinaca and AB-Pinaca/Water matrixes	[180]

ChOx: choline oxidase; MB-SPCE: Meldola Blue screen-printed carbon electrode; GLDH: enzyme glutamate dehydrogenase; CHIT: chitosan; NAD$^+$: co-factor nicotinamide adenine dinucleotide; SUA: salivary uric acid; BLE: Bluetooth Low Energy; PPD: polymerized o-phenylenediamine; Ty: tyrosinase; GOx: glucose oxidase; 4-APBA: 4-aminophenylboronic acid; PDA: polydopamine; DA: dopamine; PMNCs: polymeric nanocomposites; PB: Prussian blue; MBs: magnetic beads; PNR: polyneutral red; ADH: alcohol dehydrogenase; GA: glutaraldehyde; CS: chitosan; HRP: horseradish peroxidase; Lox: lactate oxidase; SPBGEs: basal-plane-like screen-printed graphite electrodes; FcMe: ferrocene methanol; DCHP: dicyclohexyl phthalate; AChE: acetylcholinesterase; GA: glycated albumin; FAOx: fructosyl amino acid oxidase; ε-FK: ε-fructosyllysine; PBNCs: Prussian blue nanocubes; AgNWs: silver nanowires; ChOx: cholesterol oxidase; NiO: nanostructured nickel oxide; GNR: graphene nanoribbon; RuO$_2$: ruthenium dioxide; ADH: alcohol dehydrogenase; AOx: alcohol oxidase; LOx: lactate oxidase; Cu-MOF: copper metallic framework; Pt: platinum coating; Tyr: tyrosinase; RA: rosmarinic acid; GO-SH: functionalization of graphene; PANI: polyaniline; PB: Prussian blue; ATO: antimony tin oxide; ZnONPs: zinc oxide nanoparticles; GGP: Guinea grass peroxidase; GRO: graphene oxide; PVF: polyvinylferrocene; DAOx: diamine oxidase; MAOx: monoamine oxidase; CB: carbon black; CA: cellulose acetate; DIA: diaphorase; FDH: formate dehydrogenase; DLDH: D-lactate dehydrogenase; L-LDH: L-lactate dehydrogenase; UA: uric acid; cry: Cryogel; ESD: electrospray deposition; CB: carbon black; BC: bacterial cellulose; PBNcs: Prussian blue nanocubes; MgOC: MgO-templated mesoporous carbon; GMA: glycidyl methacrylate; GMgOC: graft polymerization of GMA on the MgOC surface; E: enzyme; N: nanoparticles.

Figure 10. Schematic depicting ABs/GOx$_{ext}$/AuNPs/MBs–GOx@PDA PMNCs synthesis (adapted and reprinted with permission from [152]).

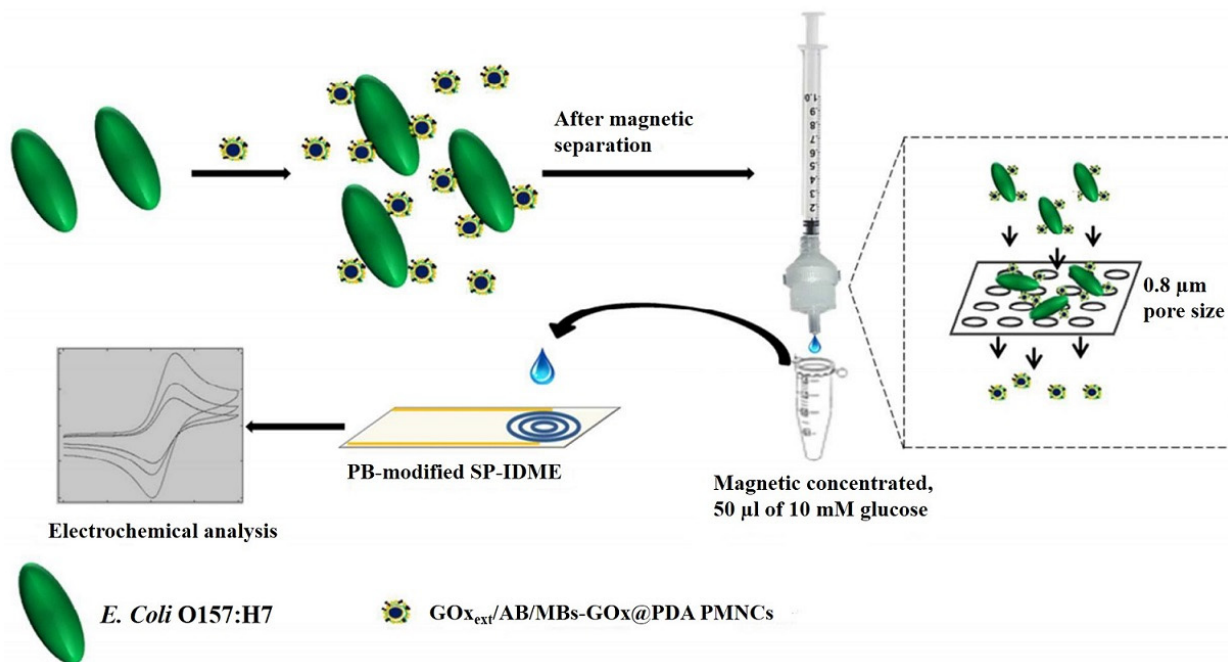**Figure 11.** Electrochemical biosensor construction for *E. coli* O157:H7 detection (adapted and reprinted with permission from [152]).
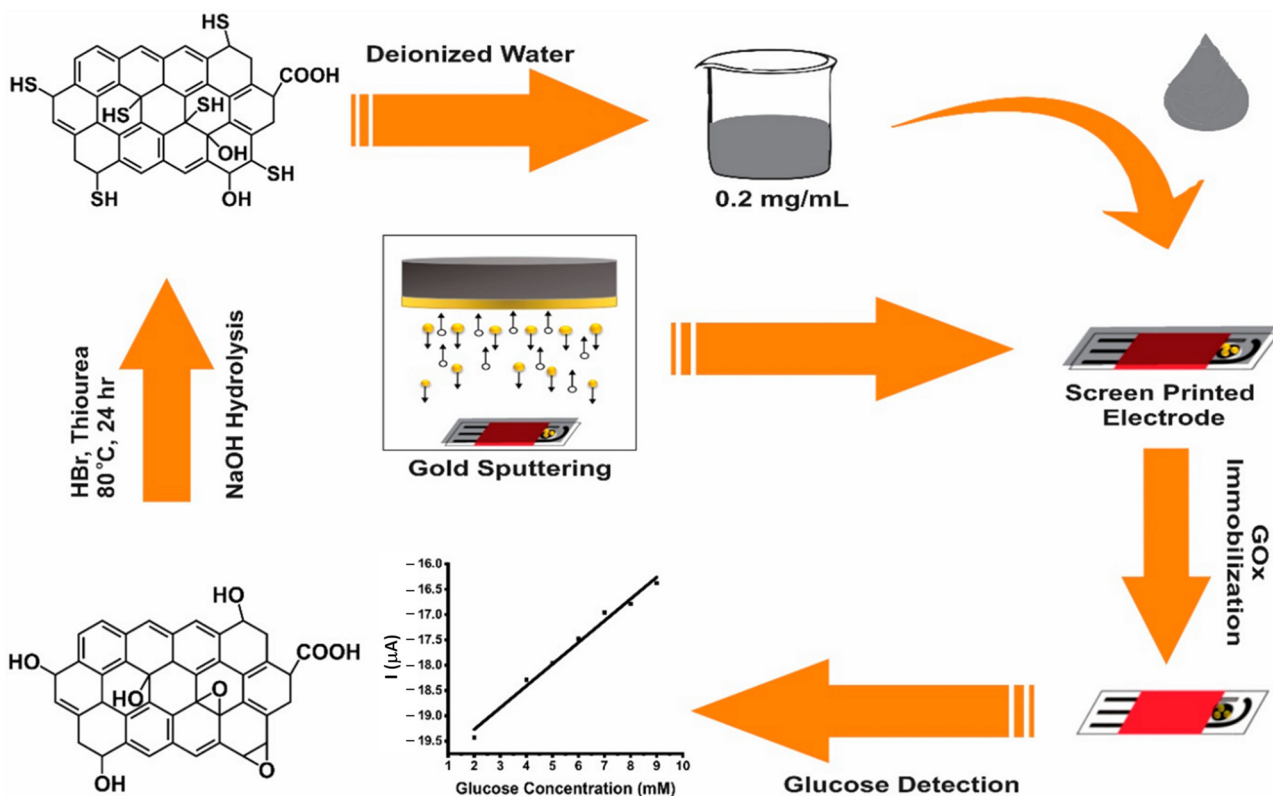

Figure 12. Schematic illustration of the GO-SH synthetic pathway to GOx-GO-SH-Au-SPE interface construction for glucose detection (adapted and reprinted with permission from [153]).
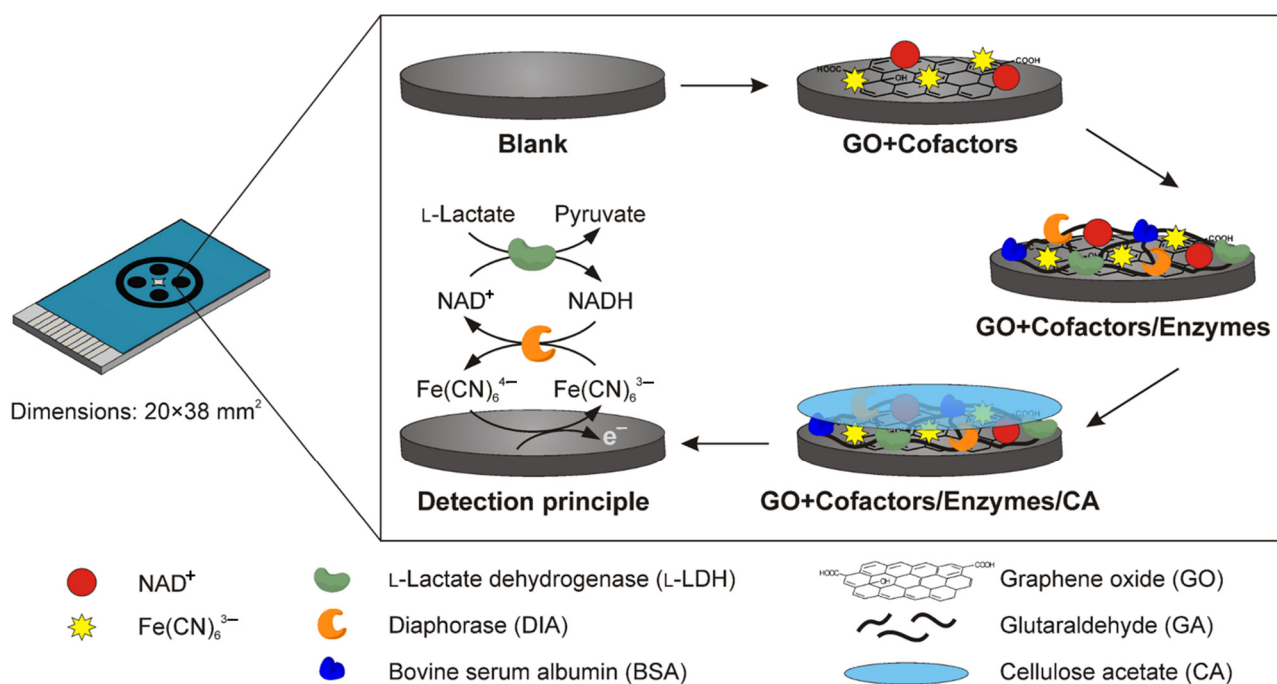
Figure 13. Schematic representation of the multianalyte SPE biosensor (adapted and reprinted with permission from [154]).

4. Conclusions

In this review, we present the most recent developments in the field of SPE-based biosensors. The modern electrochemical methods in combination with SPEs have offered advancements in micro-electronic systems. Therefore, the on-site and real-time analysis of environmental and biological compounds has significantly improved based on the miniaturization of the sensor process. Due to their cost-effectiveness and easy portability, SPEs have attracted worldwide consideration. The simple and mass production of reproducible SPEs provides the opportunity to employ SPE-based sensors as one-shot tools. SPEs' ability to be modified for the detection of numerous analytes and their cost-effectiveness have made them advantageous. Furthermore, in order to cater to specific applications, it is possible for them to be integrated into other procedures. There has recently been a growing application of SPEs as, for example, disposable biosensors, which can be employed for analyzing numerous (bio) compounds. Accordingly, to fulfil this goal, various methods have been utilized to immobilize nucleic acids, enzymes, and antibodies onto the surface of SPEs, especially for the detection of human pathogens.

Sallmonella, *E. coli*, *L. monocytogenes*, and *S. Pneumonia* were identified in various matrices with SPE-based biosensors. These electrochemical biosensors were depicted as an impressive alternative to the classical procedures for biocompound detection. In this review paper, we present the design of SPE-based biosensors and their applications for the detection of different (bio) compounds. As well, we summarize the novel SPE-based biosensor designs and their applications published in the past eight years. There has been widespread use of biosensors, including for food safety, quality control, as well as for environmental monitoring, and it is anticipated that their use will further expand in the coming years. As mentioned in this review, a variety of sensors for a wide range of analytes including alcohol, H_2O_2, neurotransmitters, glucose, DNA sensors, and immunosensors have been used for on-site detection.

The analytical applications and potential performances were significantly enhanced due to the full integration of new discoveries in nanotechnology with the new biosensors' advancements. The design of modified SPEs with the newest findings in nanomaterials, including Gr, CNTs, and AuNPs, make them suitable substrates for immobilizing biological

transducer elements. Moreover, such developments have contributed to SPEs' miniaturization by significantly increasing the sensitivity and selectivity of the sensors. This review has focused on the ways in which SPEs were biologically modified with DNA, enzymes, aptamers, and antibodies together with chemical modifications such as noble metals, enzymes, and NPs, as well as polymeric films to further enhance the performance of the biosensors for potential applications in the analysis of biocompounds.

References

1. Renedo, O.D.; Alonso-Lomillo, M.; Martínez, M.A. Recent developments in the field of screen-printed electrodes and their related applications. *Talanta* **2007**, *73*, 202–219. [CrossRef] [PubMed]
2. Ferrari, A.G.-M.; Rowley-Neale, S.J.; Banks, C.E. Screen-printed electrodes: Transitioning the laboratory in-to-the field. *Talanta Open* **2021**, *3*, 100032. [CrossRef]
3. Hart, J.P.; Wring, S.A. Recent developments in the design and application of screen-printed electrochemical sensors for biomedical, environmental and industrial analyses. *TrAC Trends Anal. Chem.* **1997**, *16*, 89–103. [CrossRef]
4. Mincu, N.-B.; Lazar, V.; Stan, D.; Mihailescu, C.M.; Iosub, R.; Mateescu, A.L. Screen-Printed Electrodes (SPE) for in vitro diagnostic purpose. *Diagnostics* **2020**, *10*, 517. [CrossRef] [PubMed]
5. Fletcher, S. Screen-Printed Carbon Electrodes. In *Electrochemistry of Carbon Electrodes*; Wiley-VCH Verlag GmbH & Co. KGaA: Weinheim, Germany, 2015; pp. 425–444. [CrossRef]
6. Li, M.; Li, Y.-T.; Li, D.-W.; Long, Y.-T. Recent developments and applications of screen-printed electrodes in environmental assays—A review. *Anal. Chim. Acta* **2012**, *734*, 31–44. [CrossRef]
7. Foster, C.W.; Kadara, R.O.; Banks, C.E. Fundamentals of screen-printing electrochemical architectures. In *Screen-Printing Electrochemical Architectures*; Springer: Cham, Switzerland, 2016; pp. 13–23. [CrossRef]
8. Couto, R.; Lima, J.; Quinaz, M. Recent developments, characteristics and potential applications of screen-printed electrodes in pharmaceutical and biological analysis. *Talanta* **2016**, *146*, 801–814. [CrossRef]
9. Arduini, F.; Micheli, L.; Moscone, D.; Palleschi, G.; Piermarini, S.; Ricci, F.; Volpe, G. Electrochemical biosensors based on nanomodified screen-printed electrodes: Recent applications in clinical analysis. *TrAC Trends Anal. Chem.* **2016**, *79*, 114–126. [CrossRef]
10. Rama, E.C.; Costa-García, A. Screen-printed electrochemical immunosensors for the detection of cancer and cardiovascular biomarkers. *Electroanalysis* **2016**, *28*, 1700–1715. [CrossRef]
11. Smart, A.; Crew, A.; Pemberton, R.; Hughes, G.; Doran, O.; Hart, J. Screen-printed carbon based biosensors and their applications in agri-food safety. *TrAC Trends Anal. Chem.* **2020**, *127*, 115898. [CrossRef]
12. Vasilescu, A.; Nunes, G.; Hayat, A.; Latif, U.; Marty, J.-L. Electrochemical affinity biosensors based on disposable screen-printed electrodes for detection of food allergens. *Sensors* **2016**, *16*, 1863. [CrossRef]
13. Mishra, R.; Nunes, G.; Souto, L.; Marty, J. Screen printed technology—An application towards biosensor development. In *Encyclopedia of Interfacial Chemistry*; Elsevier: Amsterdam, The Netherlands, 2018; pp. 487–498.
14. Hayat, A.; Marty, J.L. Disposable screen printed electrochemical sensors: Tools for environmental monitoring. *Sensors* **2014**, *14*, 10432–10453. [CrossRef] [PubMed]
15. Mohamed, H.M. Screen-printed disposable electrodes: Pharmaceutical applications and recent developments. *TrAC Trends Anal. Chem.* **2016**, *82*, 1–11. [CrossRef]
16. Metters, J.P.; Kadara, R.O.; Banks, C.E. New directions in screen printed electroanalytical sensors: An overview of recent developments. *Analyst* **2011**, *136*, 1067–1076. [CrossRef] [PubMed]
17. Li, M.; Li, D.-W.; Xiu, G.; Long, Y.-T. Applications of screen-printed electrodes in current environmental analysis. *Curr. Opin. Electrochem.* **2017**, *3*, 137–143. [CrossRef]
18. Alonso-Lomillo, M.; Domínguez-Renedo, O.; Arcos-Martínez, M. Screen-printed biosensors in microbiology; A review. *Talanta* **2010**, *82*, 1629–1636. [CrossRef]
19. Barton, J.; García, M.B.G.; Santos, D.H.; Fanjul-Bolado, P.; Ribotti, A.; McCaul, M.; Diamond, D.; Magni, P. Screen-printed electrodes for environmental monitoring of heavy metal ions: A review. *Microchim. Acta* **2016**, *183*, 503–517. [CrossRef]

20. Squissato, A.L.; Almeida, E.S.; Silva, S.G.; Richter, E.M.; Batista, A.D.; Munoz, R.A. Screen-printed electrodes for quality control of liquid (Bio) fuels. *TrAC Trends Anal. Chem.* **2018**, *108*, 210–220. [CrossRef]

21. Squissato, A.L.; Munoz, R.A.; Banks, C.E.; Richter, E.M. An overview of recent electroanalytical applications utilizing screen-printed electrodes within flow systems. *ChemElectroChem* **2020**, *7*, 2211–2221. [CrossRef]

22. Pérez-Fernández, B.; Costa-García, A.; Muñiz, A.d.l.E. Electrochemical (bio) sensors for pesticides detection using screen-printed electrodes. *Biosensors* **2020**, *10*, 32. [CrossRef]

23. Torre, R.; Costa-Rama, E.; Nouws, H.P.; Delerue-Matos, C. Screen-printed electrode-based sensors for food spoilage control: Bacteria and biogenic amines detection. *Biosensors* **2020**, *10*, 139. [CrossRef]

24. Cano-Raya, C.; Denchev, Z.Z.; Cruz, S.F.; Viana, J.C. Chemistry of solid metal-based inks and pastes for printed electronics–A review. *Appl. Mater. Today* **2019**, *15*, 416–430. [CrossRef]

25. Lanyon, Y.H.; Tothill, I.E.; Mascini, M. An amperometric bacterial biosensor based on gold screen-printed electrodes for the detection of benzene. *Anal. Lett.* **2006**, *39*, 1669–1681. [CrossRef]

26. Mistry, K.K.; Layek, K.; Mahapatra, A.; RoyChaudhuri, C.; Saha, H. A review on amperometric-type immunosensors based on screen-printed electrodes. *Analyst* **2014**, *139*, 2289–2311. [CrossRef] [PubMed]

27. Bigeleisen, J. *Screen Printing: A Contemporary Guide to the Technique of Screen Printing for Artists, Designers, and Craftsmen*; Watson-Guptill Publications Inc.: New York, NY, USA, 1971.

28. Wang, J.; Pamidi, P.V.; Rogers, K.R. Sol–gel-derived thick-film amperoEetric immunosensors. *Anal. Chem.* **1998**, *70*, 1171–1175. [CrossRef] [PubMed]

29. Sanati, A.; Jalali, M.; Raeissi, K.; Karimzadeh, F.; Kharaziha, M.; Mahshid, S.S.; Mahshid, S. A review on recent advancements in electrochemical biosensing using carbonaceous nanomaterials. *Microchim. Acta* **2019**, *186*, 773. [CrossRef]

30. Paimard, G.; Shamsipur, M.; Gholivand, M.B. A three-dimensional hybrid of CdS quantum dots/chitosan/reduced graphene oxide-based sensor for the amperometric detection of ceftazidime. *Chem. Pap.* **2022**, *77*, 437–449. [CrossRef]

31. Paimard, G.; Gholivand, M.B.; Shamsipur, M.; Ahmadi, E.; Shahlaei, M. Introduction of a thrombin sensor based on its interaction with dabigatran as an oral direct thrombin inhibitor. *Mater. Sci. Eng. C* **2021**, *119*, 111417. [CrossRef] [PubMed]

32. Fan, Z.; Ho, J.C.; Takahashi, T.; Yerushalmi, R.; Takei, K.; Ford, A.C.; Chueh, Y.L.; Javey, A. Toward the development of printable nanowire electronics and sensors. *Adv. Mater.* **2009**, *21*, 3730–3743. [CrossRef]

33. Khairy, M.; Kadara, R.O.; Banks, C.E. Electroanalytical sensing of nitrite at shallow recessed screen printed microelectrode arrays. *Anal. Methods* **2010**, *2*, 851–854. [CrossRef]

34. Kadara, R.O.; Jenkinson, N.; Banks, C.E. Screen printed recessed microelectrode arrays. *Sens. Actuators B Chem.* **2009**, *142*, 342–346. [CrossRef]

35. Fanjul-Bolado, P.; Hernández-Santos, D.; Lamas-Ardisana, P.J.; Martín-Pernía, A.; Costa-García, A. Electrochemical characterization of screen-printed and conventional carbon paste electrodes. *Electrochim. Acta* **2008**, *53*, 3635–3642. [CrossRef]

36. Foulger, S.H. Electrical properties of composites in the vicinity of the percolation threshold. *J. Appl. Polym. Sci.* **1999**, *72*, 1573–1582. [CrossRef]

37. Ahmed, M.U.; Hossain, M.M.; Safavieh, M.; Wong, Y.L.; Rahman, I.A.; Zourob, M.; Tamiya, E. Toward the development of smart and low cost point-of-care biosensors based on screen printed electrodes. *Crit. Rev. Biotechnol.* **2016**, *36*, 495–505. [CrossRef] [PubMed]

38. Sundaresan, P.; Chen, T.-W.; Chen, S.-M.; Tseng, T.-W.; Liu, X. Electrochemical activation of screen printed carbon electrode for the determination of antibiotic drug metronidazole. *Int. J. Electrochem. Sci.* **2018**, *13*, 1441–1451. [CrossRef] [PubMed]

39. Pan, D.; Rong, S.; Zhang, G.; Zhang, Y.; Zhou, Q.; Liu, F.; Li, M.; Chang, D.; Pan, H. Amperometric determination of dopamine using activated screen-printed carbon electrodes. *Electrochemistry* **2015**, *83*, 725–729. [CrossRef]

40. Bahadır, E.B.; Sezgintürk, M.K. Applications of commercial biosensors in clinical, food, environmental, and biothreat/biowarfare analyses. *Anal. Biochem.* **2015**, *478*, 107–120. [CrossRef]

41. Scognamiglio, V. Nanotechnology in glucose monitoring: Advances and challenges in the last 10 years. *Biosens. Bioelectron.* **2013**, *47*, 12–25. [CrossRef]

42. Arduini, F.; Forchielli, M.; Amine, A.; Neagu, D.; Cacciotti, I.; Nanni, F.; Moscone, D.; Palleschi, G. Screen-printed biosensor modified with carbon black nanoparticles for the determination of paraoxon based on the inhibition of butyrylcholinesterase. *Microchim. Acta* **2015**, *182*, 643–651. [CrossRef]

43. Cinti, S.; Arduini, F.; Carbone, M.; Sansone, L.; Cacciotti, I.; Moscone, D.; Palleschi, G. Screen-printed electrodes modified with carbon nanomaterials: A comparison among carbon black, carbon nanotubes and graphene. *Electroanalysis* **2015**, *27*, 2230–2238. [CrossRef]

44. Putzbach, W.; Ronkainen, N.J. Immobilization techniques in the fabrication of nanomaterial-based electrochemical biosensors: A review. *Sensors* **2013**, *13*, 4811–4840. [CrossRef]

45. Antuña-Jiménez, D.; González-García, M.B.; Hernández-Santos, D.; Fanjul-Bolado, P. Screen-printed electrodes modified with metal nanoparticles for small molecule sensing. *Biosensors* **2020**, *10*, 9. [CrossRef] [PubMed]

46. Duffy, G.; Moore, E. Electrochemical immunosensors for food analysis: A review of recent developments. *Anal. Lett.* **2017**, *50*, 1–32. [CrossRef]

47. Chu, Z.; Peng, J.; Jin, W. Advanced nanomaterial inks for screen-printed chemical sensors. *Sens. Actuators B Chem.* **2017**, *243*, 919–926. [CrossRef]

48. Thiyagarajan, N.; Chang, J.-L.; Senthilkumar, K.; Zen, J.-M. Disposable electrochemical sensors: A mini review. *Electrochem. Commun.* **2014**, *38*, 86–90. [CrossRef]

49. Banks, C.E.; Crossley, A.; Salter, C.; Wilkins, S.J.; Compton, R.G. Carbon nanotubes contain metal impurities which are responsible for the "electrocatalysis" seen at some nanotube-modified electrodes. *Angew. Chem. Int. Ed.* **2006**, *45*, 2533–2537. [CrossRef]

50. Yang, Y.; Asiri, A.M.; Tang, Z.; Du, D.; Lin, Y. Graphene based materials for biomedical applications. *Mater. Today* **2013**, *16*, 365–373. [CrossRef]

51. Díaz-Cruz, J.M.; Serrano, N.; Pérez-Ràfols, C.; Ariño, C.; Esteban, M. Electroanalysis from the past to the twenty-first century: Challenges and perspectives. *J. Solid State Electrochem.* **2020**, *24*, 2653–2661. [CrossRef]

52. Kim, J.; Campbell, A.S.; Wang, J. Wearable non-invasive epidermal glucose sensors: A review. *Talanta* **2018**, *177*, 163–170. [CrossRef]

53. Campbell, A.S.; Kim, J.; Wang, J. Wearable electrochemical alcohol biosensors. *Curr. Opin. Electrochem.* **2018**, *10*, 126–135. [CrossRef]

54. Cao, L.; Fang, C.; Zeng, R.; Zhao, X.; Zhao, F.; Jiang, Y.; Chen, Z. A disposable paper-based microfluidic immunosensor based on reduced graphene oxide-tetraethylene pentamine/Au nanocomposite decorated carbon screen-printed electrodes. *Sens. Actuators B Chem.* **2017**, *252*, 44–54. [CrossRef]

55. Shriver-Lake, L.C.; Zabetakis, D.; Dressick, W.J.; Stenger, D.A.; Trammell, S.A. based electrochemical detection of chlorate. *Sensors* **2018**, *18*, 328. [CrossRef] [PubMed]

56. Colozza, N.; Kehe, K.; Dionisi, G.; Popp, T.; Tsoutsoulopoulos, A.; Steinritz, D.; Moscone, D.; Arduini, F. A wearable origami-like paper-based electrochemical biosensor for sulfur mustard detection. *Biosens. Bioelectron.* **2019**, *129*, 15–23. [CrossRef] [PubMed]

57. Figueredo, F.; Jesús González-Pabón, M.; Cortón, E. Low Cost Layer by Layer Construction of CNT/Chitosan Flexible Paper-based Electrodes: A Versatile Electrochemical Platform for Point of Care and Point of Need Testing. *Electroanalysis* **2018**, *30*, 497–508. [CrossRef]

58. Wang, P.; Wang, M.; Zhou, F.; Yang, G.; Qu, L.; Miao, X. Development of a paper-based, inexpensive, and disposable electrochemical sensing platform for nitrite detection. *Electrochem. Commun.* **2017**, *81*, 74–78. [CrossRef]

59. Jaiswal, N.; Tiwari, I. Recent build outs in electroanalytical biosensors based on carbon-nanomaterial modified screen printed electrode platforms. *Anal. Methods* **2017**, *9*, 3895–3907. [CrossRef]

60. Thévenot, D.R.; Toth, K.; Durst, R.A.; Wilson, G.S. Electrochemical biosensors: Recommended definitions and classification. *Biosens. Bioelectron.* **2001**, *16*, 121–131. [CrossRef]

61. Honeychurch, K.C.; Hart, J.P. Screen-printed electrochemical sensors for monitoring metal pollutants. *TrAC Trends Anal. Chem.* **2003**, *22*, 456–469. [CrossRef]

62. Lucarelli, F.; Marrazza, G.; Turner, A.P.; Mascini, M. Carbon and gold electrodes as electrochemical transducers for DNA hybridisation sensors. *Biosens. Bioelectron.* **2004**, *19*, 515–530. [CrossRef]

63. Ricci, F.; Plaxco, K.W. E-DNA sensors for convenient, label-free electrochemical detection of hybridization. *Microchim. Acta* **2008**, *163*, 149–155. [CrossRef]

64. Palchetti, I.; Mascini, M. Electrochemical nanomaterial-based nucleic acid aptasensors. *Anal. Bioanal. Chem.* **2012**, *402*, 3103–3114. [CrossRef]

65. Biagiotti, V.; Porchetta, A.; Desiderati, S.; Plaxco, K.W.; Palleschi, G.; Ricci, F. Probe accessibility effects on the performance of electrochemical biosensors employing DNA monolayers. *Anal. Bioanal. Chem.* **2012**, *402*, 413–421. [CrossRef] [PubMed]

66. Kokkinos, C.; Prodromidis, M.; Economou, A.; Petrou, P.; Kakabakos, S. Quantum dot-based electrochemical DNA biosensor using a screen-printed graphite surface with embedded bismuth precursor. *Electrochem. Commun.* **2015**, *60*, 47–51. [CrossRef]

67. Abd Rashid, J.I.; Yusof, N.A.; Abdullah, J.; Hashim, U.; Hajian, R. A novel disposable biosensor based on SiNWs/AuNPs modified-screen printed electrode for dengue virus DNA oligomer detection. *IEEE Sens. J.* **2015**, *15*, 4420–4427. [CrossRef]

68. Tortolini, C.; Bollella, P.; Antonelli, M.L.; Antiochia, R.; Mazzei, F.; Favero, G. DNA-based biosensors for Hg^{2+} determination by polythymine–methylene blue modified electrodes. *Biosens. Bioelectron.* **2015**, *67*, 524–531. [CrossRef]

69. Erdem, A.; Eksin, E.; Congur, G. Indicator-free electrochemical biosensor for microRNA detection based on carbon nanofibers modified screen printed electrodes. *J. Electroanal. Chem.* **2015**, *755*, 167–173. [CrossRef]

70. Zhang, Y.; Geng, X.; Ai, J.; Gao, Q.; Qi, H.; Zhang, C. Signal amplification detection of DNA using a sensor fabricated by one-step covalent immobilization of amino-terminated probe DNA onto the polydopamine-modified screen-printed carbon electrode. *Sens. Actuators B Chem.* **2015**, *221*, 1535–1541. [CrossRef]

71. Malecka, K.; Stachyra, A.; Góra-Sochacka, A.; Sirko, A.; Zagórski-Ostoja, W.; Radecka, H.; Radecki, J. Electrochemical genosensor based on disc and screen printed gold electrodes for detection of specific DNA and RNA sequences derived from Avian Influenza Virus H5N1. *Sens. Actuators B Chem.* **2016**, *224*, 290–297. [CrossRef]

72. Mazloum-Ardakani, M.; Hosseinzadeh, L.; Heidari, M.M. Detection of the M268T Angiotensinogen A3B2 mutation gene based on screen-printed electrodes modified with a nanocomposite: Application to human genomic samples. *Microchim. Acta* **2016**, *183*, 219–227. [CrossRef]

73. Ilkhani, H.; Farhad, S. A novel electrochemical DNA biosensor for Ebola virus detection. *Anal. Biochem.* **2018**, *557*, 151–155. [CrossRef]

74. Shoaie, N.; Forouzandeh, M.; Omidfar, K. Voltammetric determination of the Escherichia coli DNA using a screen-printed carbon electrode modified with polyaniline and gold nanoparticles. *Microchim. Acta* **2018**, *185*, 217. [CrossRef]

75. Uygun, Z.O.; Atay, S. Label-free highly sensitive detection of DNA approximate length and concentration by impedimetric CRISPR-dCas9 based biosensor technology. *Bioelectrochemistry* **2021**, *140*, 107812. [CrossRef] [PubMed]

76. Karadurmus, L.; Dogan-Topal, B.; Kurbanoglu, S.; Shah, A.; Ozkan, S.A. The interaction between DNA and three intercalating anthracyclines using electrochemical DNA nanobiosensor based on metal nanoparticles modified screen-printed electrode. *Micromachines* **2021**, *12*, 1337. [CrossRef] [PubMed]

77. Thoeny, V.; Melnik, E.; Asadi, M.; Mehrabi, P.; Schalkhammer, T.; Pulverer, W.; Maier, T.; Mutinati, G.C.; Lieberzeit, P.; Hainberger, R. Detection of breast cancer-related point-mutations using screen-printed and gold-plated electrochemical sensor arrays suitable for point-of-care applications. *Talanta Open* **2022**, *6*, 100150. [CrossRef]

78. Chai, H.; Ma, X.; Sun, H.; Miao, P. DNA–MnO_2 Nanoconjugates Investigation and Application for Electrochemical Polymerase Chain Reaction. *Anal. Chem.* **2022**, *94*, 4565–4569. [CrossRef] [PubMed]

79. Zhang, W.; Zhang, P.; Liang, Y.; Cheng, W.; Li, L.; Wang, H.; Yu, Z.; Liu, Y.; Zhang, X. Rapid electrochemical quantification of trace Hg^{2+} using a hairpin DNA probe and quantum dot modified screen-printed gold electrodes. *RSC Adv.* **2022**, *12*, 13448–13455. [CrossRef] [PubMed]

80. Abedi, R.; Raoof, J.B.; Hashkavayi, A.B.; Asghari, M.; Azimi, R.; Hejazi, M.S. A novel genosensor based on Fe_3O_4@SiO_2/DABCO-modified screen-printed graphite electrode for detection of prostate cancer gene sequence hybridization. *J. Iran. Chem. Soc.* **2022**, *19*, 2631–2640. [CrossRef]

81. Becker, J.M.; Lielpetere, A.; Szczesny, J.; Ruff, A.; Conzuelo, F.; Schuhmann, W. Assembling a Low-volume Biofuel Cell on a Screen-printed Electrode for Glucose Sensing. *Electroanalysis* **2022**, *34*, 1629–1637. [CrossRef]

82. Aghaei, F.; Seifati, S.M.; Nasirizadeh, N. Development of a DNA biosensor for the detection of phenylketonuria based on a screen-printed gold electrode and hematoxylin. *Anal. Methods* **2017**, *9*, 966–973. [CrossRef]

83. Huang, K.-J.; Liu, Y.-J.; Zhang, J.-Z.; Liu, Y.-M. A novel aptamer sensor based on layered tungsten disulfide nanosheets and Au nanoparticles amplification for 17β-estradiol detection. *Anal. Methods* **2014**, *6*, 8011–8017. [CrossRef]

84. Mirian, M.; Khanahmad, H.; Darzi, L.; Salehi, M.; Sadeghi-Aliabadi, H. Oligonucleotide aptamers: Potential novel molecules against viral hepatitis. *Res. Pharm. Sci.* **2017**, *12*, 88. [CrossRef]

85. Ilgu, M.; Nilsen-Hamilton, M. Aptamers in analytics. *Analyst* **2016**, *141*, 1551–1568. [CrossRef] [PubMed]

86. Douaki, A.; Garoli, D.; Inam, A.S.; Angeli, M.A.C.; Cantarella, G.; Rocchia, W.; Wang, J.; Petti, L.; Lugli, P. Smart Approach for the Design of Highly Selective Aptamer-Based Biosensors. *Biosensors* **2022**, *12*, 574. [CrossRef] [PubMed]

87. Mishra, G.K.; Sharma, V.; Mishra, R.K. Electrochemical aptasensors for food and environmental safeguarding: A review. *Biosensors* **2018**, *8*, 28. [CrossRef] [PubMed]

88. Ren, C.; Li, H.; Lu, X.; Qian, J.; Zhu, M.; Chen, W.; Liu, Q.; Hao, N.; Li, H.; Wang, K. A disposable aptasensing device for label-free detection of fumonisin B1 by integrating PDMS film-based micro-cell and screen-printed carbon electrode. *Sens. Actuators B Chem.* **2017**, *251*, 192–199. [CrossRef]

89. Wang, X.; Su, J.; Zeng, D.; Liu, G.; Liu, L.; Xu, Y.; Wang, C.; Liu, X.; Wang, L.; Mi, X. Gold nano-flowers (Au NFs) modified screen-printed carbon electrode electrochemical biosensor for label-free and quantitative detection of glycated hemoglobin. *Talanta* **2019**, *201*, 119–125. [CrossRef]

90. Santharaman, P.; Venkatesh, K.A.; Vairamani, K.; Benjamin, A.R.; Sethy, N.K.; Bhargava, K.; Karunakaran, C. ARM-microcontroller based portable nitrite electrochemical analyzer using cytochrome c reductase biofunctionalized onto screen printed carbon electrode. *Biosens. Bioelectron.* **2017**, *90*, 410–417. [CrossRef]

91. Eissa, S.; Almusharraf, A.Y.; Zourob, M. A comparison of the performance of voltammetric aptasensors for glycated haemoglobin on different carbon nanomaterials-modified screen printed electrodes. *Mater. Sci. Eng. C* **2019**, *101*, 423–430. [CrossRef]

92. Zhang, D.; Jiang, J.; Chen, J.; Zhang, Q.; Lu, Y.; Yao, Y.; Li, S.; Liu, G.L.; Liu, Q. Smartphone-based portable biosensing system using impedance measurement with printed electrodes for 2,4,6-trinitrotoluene (TNT) detection. *Biosens. Bioelectron.* **2015**, *70*, 81–88. [CrossRef]

93. Martín-Yerga, D.; Carrasco-Rodríguez, J.; Alonso, F.J.G.; Costa-García, A. Competitive electrochemical biosensing of biotin using cadmium-modified titanium phosphate nanoparticles and 8-channel screen-printed disposable electrodes. *Anal. Methods* **2017**, *9*, 3983–3991. [CrossRef]

94. Li, Y.; Ran, G.; Lu, G.; Ni, X.; Liu, D.; Sun, J.; Xie, C.; Yao, D.; Bai, W. Highly sensitive label-free electrochemical aptasensor based on screen-printed electrode for detection of cadmium (II) ions. *J. Electrochem. Soc.* **2019**, *166*, B449. [CrossRef]

95. Vasudevan, M.; Tai, M.J.; Perumal, V.; Gopinath, S.C.; Murthe, S.S.; Ovinis, M.; Mohamed, N.M.; Joshi, N. Highly sensitive and selective acute myocardial infarction detection using aptamer-tethered MoS_2 nanoflower and screen-printed electrodes. *Biotechnol. Appl. Biochem.* **2021**, *68*, 1386–1395.

96. Jo, H.; Her, J.; Lee, H.; Shim, Y.-B.; Ban, C. Highly sensitive amperometric detection of cardiac troponin I using sandwich aptamers and screen-printed carbon electrodes. *Talanta* **2017**, *165*, 442–448. [CrossRef] [PubMed]

97. Bagheri Hashkavayi, A.; Bakhsh Raoof, J.; Ojani, R.; Hamidi Asl, E. Label-free electrochemical aptasensor for determination of chloramphenicol based on gold nanocubes-modified screen-printed gold electrode. *Electroanalysis* **2015**, *27*, 1449–1456. [CrossRef]

98. Tabrizi, M.A.; Shamsipur, M.; Saber, R.; Sarkar, S. Simultaneous determination of CYC and VEGF165 tumor markers based on immobilization of flavin adenine dinucleotide and thionine as probes on reduced graphene oxide-poly (amidoamine)/gold nanocomposite modified dual working screen-printed electrode. *Sens. Actuators B Chem.* **2017**, *240*, 1174–1181. [CrossRef]

99. Hashkavayi, A.B.; Raoof, J.B. Design an aptasensor based on structure-switching aptamer on dendritic gold nanostructures/ Fe_3O_4@SiO_2/DABCO modified screen printed electrode for highly selective detection of epirubicin. *Biosens. Bioelectron.* **2017**, *91*, 650–657. [CrossRef]

100. Ahmadi, A.; Khoshfetrat, S.M.; Kabiri, S.; Dorraji, P.S.; Larijani, B.; Omidfar, K. Electrochemiluminescence paper-based screen-printed electrode for HbA1c detection using two-dimensional zirconium metal-organic framework/Fe_3O_4 nanosheet composites decorated with Au nanoclusters. *Microchim. Acta* **2021**, *188*, 296. [CrossRef]

101. Park, K. Impedance Technique-Based Label-Free Electrochemical Aptasensor for Thrombin Using Single-Walled Carbon Nanotubes-Casted Screen-Printed Carbon Electrode. *Sensors* **2022**, *22*, 2699. [CrossRef]

102. Gómez-Arconada, L.; Díaz-Fernández, A.; Ferapontova, E.E. Ultrasensitive disposable apatasensor for reagentless electrocatalytic detection of thrombin: An O_2-Dependent hemin-G4-aptamer assay on gold screen-printed electrodes. *Talanta* **2022**, *245*, 123456. [CrossRef]

103. Amouzadeh Tabrizi, M.; Acedo, P. An electrochemical impedance spectroscopy-based aptasensor for the determination of SARS-CoV-2-RBD using a carbon nanofiber–gold nanocomposite modified screen-printed electrode. *Biosensors* **2022**, *12*, 142. [CrossRef]

104. Curti, F.; Fortunati, S.; Knoll, W.; Giannetto, M.; Corradini, R.; Bertucci, A.; Careri, M. A Folding-Based Electrochemical Aptasensor for the Single-Step Detection of the SARS-CoV-2 Spike Protein. *ACS Appl. Mater. Interfaces* **2022**, *14*, 19204–19211. [CrossRef]

105. Hassani, S.; Akmal, M.R.; Salek-Maghsoudi, A.; Rahmani, S.; Ganjali, M.R.; Norouzi, P.; Abdollahi, M. Novel label-free electrochemical aptasensor for determination of Diazinon using gold nanoparticles-modified screen-printed gold electrode. *Biosens. Bioelectron.* **2018**, *120*, 122–128. [CrossRef] [PubMed]

106. Ferreira, D.C.; Batistuti, M.R.; Junior, B.B.; Mulato, M. Aptasensor based on screen-printed electrode for breast cancer detection in undiluted human serum. *Bioelectrochemistry* **2021**, *137*, 107586. [CrossRef] [PubMed]

107. Amouzadeh Tabrizi, M.; Shamsipur, M.; Saber, R.; Sarkar, S.; Besharati, M. An electrochemical aptamer-based assay for femtomolar determination of insulin using a screen printed electrode modified with mesoporous carbon and 1,3,6,8-pyrenetetrasulfonate. *Microchim. Acta* **2018**, *185*, 59. [CrossRef] [PubMed]

108. Rahmati, Z.; Roushani, M.; Hosseini, H.; Choobin, H. Label-free electrochemical aptasensor for rapid detection of SARS-CoV-2 spike glycoprotein based on the composite of $Cu(OH)_2$ nanorods arrays as a high-performance surface substrate. *Bioelectrochemistry* **2022**, *146*, 108106. [CrossRef] [PubMed]

109. Villalonga, A.; Sánchez, A.; Vilela, D.; Mayol, B.; Martínez-Ruíz, P.; Villalonga, R. Electrochemical aptasensor based on anisotropically modified (Janus-type) gold nanoparticles for determination of C-reactive protein. *Microchim. Acta* **2022**, *189*, 309. [CrossRef] [PubMed]

110. Şahin, S.; Kaya, Ş.; Üstündağ, Z.; Caglayan, M.O. An electrochemical signal switch–based (on–off) aptasensor for sensitive detection of insulin on gold-deposited screen-printed electrodes. *J. Solid State Electrochem.* **2022**, *26*, 907–915. [CrossRef]

111. Pakzad, M.; Fouladdel, S.; Nili-Ahmadabadi, A.; Pourkhalili, N.; Baeeri, M.; Azizi, E.; Sabzevari, O.; Ostad, S.N.; Abdollahi, M. Sublethal exposures of diazinon alters glucose homostasis in Wistar rats: Biochemical and molecular evidences of oxidative stress in adipose tissues. *Pestic. Biochem. Physiol.* **2013**, *105*, 57–61. [CrossRef]

112. Zhou, Q.; Sun, X.; Gao, R.; Hu, J. Mechanism and kinetic properties for OH-initiated atmospheric degradation of the organophosphorus pesticide diazinon. *Atmos. Environ.* **2011**, *45*, 3141–3148. [CrossRef]

113. Bhattacharjee, S.; Fakhruddin, A.; Chowdhury, M.; Rahman, M.; Alam, M. Monitoring of selected pesticides residue levels in water samples of paddy fields and removal of cypermethrin and chlorpyrifos residues from water using rice bran. *Bull. Environ. Contam. Toxicol.* **2012**, *89*, 348–353. [CrossRef]

114. Akan, J.; Jafiya, L.; Mohammed, Z.; Abdulrahman, F. Organophosphorus pesticide residues in vegetables and soil samples from alau dam and gongulong agricultural areas, Borno State, Nigeria. *Ecosystems* **2013**, *3*, 58–64. [CrossRef]

115. Yalow, R.S.; Berson, S.A. Assay of plasma insulin in human subjects by immunological methods. *Nature* **1959**, *184*, 1648–1649. [CrossRef]

116. Clark, L.C., Jr.; Lyons, C. Electrode systems for continuous monitoring in cardiovascular surgery. *Ann. N. Y. Acad. Sci.* **1962**, *102*, 29–45. [CrossRef]

117. Ricci, F.; Volpe, G.; Micheli, L.; Palleschi, G. A review on novel developments and applications of immunosensors in food analysis. *Anal. Chim. Acta* **2007**, *605*, 111–129. [CrossRef] [PubMed]

118. Escamilla-Gómez, V.; Campuzano, S.; Pedrero, M.; Pingarrón, J.M. Gold screen-printed-based impedimetric immunobiosensors for direct and sensitive Escherichia coli quantisation. *Biosens. Bioelectron.* **2009**, *24*, 3365–3371. [CrossRef] [PubMed]

119. Taleat, Z.; Khoshroo, A.; Mazloum-Ardakani, M. Screen-printed electrodes for biosensing: A review (2008–2013). *Microchim. Acta* **2014**, *181*, 865–891. [CrossRef]

120. Lien, T.T.; Takamura, Y.; Tamiya, E.; Mun'delanji, C.V. Modified screen printed electrode for development of a highly sensitive label-free impedimetric immunosensor to detect amyloid beta peptides. *Anal. Chim. Acta* **2015**, *892*, 69–76. [CrossRef] [PubMed]

121. Martin-Yerga, D.; Costa-Garcia, A. Towards a blocking-free electrochemical immunosensing strategy for anti-transglutaminase antibodies using screen-printed electrodes. *Bioelectrochemistry* **2015**, *105*, 88–94. [CrossRef] [PubMed]

122. Fei, J.; Dou, W.; Zhao, G. A sandwich electrochemical immunoassay for Salmonella pullorum and Salmonella gallinarum based on a $AuNPs/SiO_2/Fe_3O_4$ adsorbing antibody and 4 channel screen printed carbon electrode electrodeposited gold nanoparticles. *RSC Adv.* **2015**, *5*, 74548–74556. [CrossRef]

123. Tsai, J.-Z.; Chen, C.-J.; Settu, K.; Lin, Y.-F.; Chen, C.-L.; Liu, J.-T. Screen-printed carbon electrode-based electrochemical immunosensor for rapid detection of microalbuminuria. *Biosens. Bioelectron.* **2016**, *77*, 1175–1182. [CrossRef]

124. Chan, K.; Lim, H.; Shams, N.; Jayabal, S.; Pandikumar, A.; Huang, N. Fabrication of graphene/gold-modified screen-printed electrode for detection of carcinoembryonic antigen. *Mater. Sci. Eng. C* **2016**, *58*, 666–674. [CrossRef]

125. Moreira, F.T.; Ferreira, M.J.M.; Puga, J.R.; Sales, M.G.F. Screen-printed electrode produced by printed-circuit board technology. Application to cancer biomarker detection by means of plastic antibody as sensing material. *Sens. Actuators B Chem.* **2016**, *223*, 927–935. [CrossRef] [PubMed]

126. Mehta, J.; Vinayak, P.; Tuteja, S.K.; Chhabra, V.A.; Bhardwaj, N.; Paul, A.; Kim, K.-H.; Deep, A. Graphene modified screen printed immunosensor for highly sensitive detection of parathion. *Biosens. Bioelectron.* **2016**, *83*, 339–346. [CrossRef] [PubMed]

127. Lin, C.-H.; Wu, C.-C.; Kuo, Y.-F. A high sensitive impedimetric salbutamol immunosensor based on the gold nanostructure-deposited screen-printed carbon electrode. *J. Electroanal. Chem.* **2016**, *768*, 27–33. [CrossRef]

128. Lee, S.; Lim, H.; Ibrahim, I.; Jamil, A.; Pandikumar, A.; Huang, N. Horseradish peroxidase-labeled silver/reduced graphene oxide thin film-modified screen-printed electrode for detection of carcinoembryonic antigen. *Biosens. Bioelectron.* **2017**, *89*, 673–680. [CrossRef] [PubMed]

129. Tallapragada, S.D.; Layek, K.; Mukherjee, R.; Mistry, K.K.; Ghosh, M. Development of screen-printed electrode based immunosensor for the detection of HER2 antigen in human serum samples. *Bioelectrochemistry* **2017**, *118*, 25–30. [CrossRef]

130. Jampasa, S.; Siangproh, W.; Laocharoensuk, R.; Vilaivan, T.; Chailapakul, O. Electrochemical detection of c-reactive protein based on anthraquinone-labeled antibody using a screen-printed graphene electrode. *Talanta* **2018**, *183*, 311–319. [CrossRef]

131. Zhao, L.; Han, H.; Ma, Z. Improved screen-printed carbon electrode for multiplexed label-free amperometric immuniosensor: Addressing its conductivity and reproducibility challenges. *Biosens. Bioelectron.* **2018**, *101*, 304–310. [CrossRef]

132. Rodovalho, V.; Araujo, G.; Vaz, E.; Ueira-Vieira, C.; Goulart, L.; Madurro, J.; Brito-Madurro, A. Peptide-based electrochemical biosensor for juvenile idiopathic arthritis detection. *Biosens. Bioelectron.* **2018**, *100*, 577–582. [CrossRef]

133. Johari-Ahar, M.; Karami, P.; Ghanei, M.; Afkhami, A.; Bagheri, H. Development of a molecularly imprinted polymer tailored on disposable screen-printed electrodes for dual detection of EGFR and VEGF using nano-liposomal amplification strategy. *Biosens. Bioelectron.* **2018**, *107*, 26–33. [CrossRef]

134. Mo, X.; Wu, Z.; Huang, J.; Zhao, G.; Dou, W. A sensitive and regenerative electrochemical immunosensor for quantitative detection of Escherichia coli O157: H7 based on stable polyaniline coated screen-printed carbon electrode and rGO-NR-Au@Pt. *Anal. Methods* **2019**, *11*, 1475–1482. [CrossRef]

135. Phetsang, S.; Jakmunee, J.; Mungkornasawakul, P.; Laocharoensuk, R.; Ounnunkad, K. Sensitive amperometric biosensors for detection of glucose and cholesterol using a platinum/reduced graphene oxide/poly (3-aminobenzoic acid) film-modified screen-printed carbon electrode. *Bioelectrochemistry* **2019**, *127*, 125–135. [CrossRef] [PubMed]

136. Viet, N.X.; Hoan, N.X.; Takamura, Y. Development of highly sensitive electrochemical immunosensor based on single-walled carbon nanotube modified screen-printed carbon electrode. *Mater. Chem. Phys.* **2019**, *227*, 123–129. [CrossRef]

137. Thunkhamrak, C.; Chuntib, P.; Ounnunkad, K.; Banet, P.; Aubert, P.-H.; Saianand, G.; Gopalan, A.-I.; Jakmunee, J. Highly sensitive voltammetric immunosensor for the detection of prostate specific antigen based on silver nanoprobe assisted graphene oxide modified screen printed carbon electrode. *Talanta* **2020**, *208*, 120389. [CrossRef] [PubMed]

138. Khue, V.Q.; Huy, T.Q.; Phan, V.N.; Tuan-Le, A.; Le, D.T.T.; Tonezzer, M.; Hanh, N.T.H. Electrochemical stability of screen-printed electrodes modified with Au nanoparticles for detection of methicillin-resistant Staphylococcus aureus. *Mater. Chem. Phys.* **2020**, *255*, 123562. [CrossRef]

139. Fabiani, L.; Saroglia, M.; Galatà, G.; De Santis, R.; Fillo, S.; Luca, V.; Faggioni, G.; D'Amore, N.; Regalbuto, E.; Salvatori, P. Magnetic beads combined with carbon black-based screen-printed electrodes for COVID-19: A reliable and miniaturized electrochemical immunosensor for SARS-CoV-2 detection in saliva. *Biosens. Bioelectron.* **2021**, *171*, 112686. [CrossRef] [PubMed]

140. Martins, T.S.; Bott-Neto, J.L.; Machado, S.A.; Oliveira, O.N., Jr. Label-Free Electrochemical Immunosensor Made with Tree-like Gold Dendrites for Monitoring 25-Hydroxyvitamin D3 Metabolite. *ACS Appl. Mater. Interfaces* **2022**, *14*, 31455–31462. [CrossRef]

141. Mehmandoust, M.; Erk, E.E.; Soylak, M.; Erk, N.; Karimi, F. Metal–Organic Framework Based Electrochemical Immunosensor for Label-Free Detection of Glial Fibrillary Acidic Protein as a Biomarker. *Ind. Eng. Chem. Res.* **2022**. [CrossRef]

142. Jafari, S.; Burr, L.; Migliorelli, D.; Galve, R.; Marco, M.-P.; Campbell, K.; Elliott, C.; Suman, M.; Sturla, S.J.; Generelli, S. Smartphone-based magneto-immunosensor on carbon black modified screen-printed electrodes for point-of-need detection of aflatoxin B1 in cereals. *Anal. Chim. Acta* **2022**, *1221*, 340118. [CrossRef]

143. Jiang, F.; Xiao, Z.; Wang, T.; Wang, J.; Bie, L.; Saleh, L.; Frey, K.; Zhang, L.; Wang, J. Rapid and sensitive multiplex detection of COVID-19 antigens and antibody using electrochemical immunosensor-/aptasensor-enabled biochips. *Chem. Commun.* **2022**, *58*, 7285–7288. [CrossRef]

144. Polli, F.; D'Agostino, C.; Zumpano, R.; De Martino, V.; Favero, G.; Colangelo, L.; Minisola, S.; Mazzei, F. ASu@MNPs-based electrochemical immunosensor for vitamin D3 serum samples analysis. *Talanta* **2023**, *251*, 123755. [CrossRef]

145. Du, D.; Wang, J.; Lu, D.; Dohnalkova, A.; Lin, Y. Multiplexed electrochemical immunoassay of phosphorylated proteins based on enzyme-functionalized gold nanorod labels and electric field-driven acceleration. *Anal. Chem.* **2011**, *83*, 6580–6585. [CrossRef] [PubMed]

146. Wan, Y.; Zhou, Y.G.; Poudineh, M.; Safaei, T.S.; Mohamadi, R.M.; Sargent, E.H.; Kelley, S.O. Highly specific electrochemical analysis of cancer cells using multi-nanoparticle labeling. *Angew. Chem.* **2014**, *126*, 13361–13365. [CrossRef]

147. Agrisuelas, J.; González-Sánchez, M.-I.; Valero, E. Hydrogen peroxide sensor based on in situ grown Pt nanoparticles from waste screen-printed electrodes. *Sens. Actuators B Chem.* **2017**, *249*, 499–505. [CrossRef]

148. Sassolas, A.; Blum, L.J.; Leca-Bouvier, B.D. Immobilization strategies to develop enzymatic biosensors. *Biotechnol. Adv.* **2012**, *30*, 489–511. [CrossRef]

149. Malmiri, H.J.; Jahanian, M.A.G.; Berenjian, A. Potential applications of chitosan nanoparticles as novel support in enzyme immobilization. *Am. J. Biochem. Biotechnol.* **2012**, *8*, 203–219.

150. Qian, L.; Yang, X. Composite film of carbon nanotubes and chitosan for preparation of amperometric hydrogen peroxide biosensor. *Talanta* **2006**, *68*, 721–727. [CrossRef] [PubMed]

151. Hughes, G.; Pemberton, R.; Fielden, P.; Hart, J.P. Development of a novel reagentless, screen-printed amperometric biosensor based on glutamate dehydrogenase and NAD+, integrated with multi-walled carbon nanotubes for the determination of glutamate in food and clinical applications. *Sens. Actuators B Chem.* **2015**, *216*, 614–621. [CrossRef]

152. Xu, M.; Wang, R.; Li, Y. An electrochemical biosensor for rapid detection of E. coli O157: H7 with highly efficient bi-functional glucose oxidase-polydopamine nanocomposites and Prussian blue modified screen-printed interdigitated electrodes. *Analyst* **2016**, *141*, 5441–5449. [CrossRef]

153. Akhtar, M.A.; Batool, R.; Hayat, A.; Han, D.; Riaz, S.; Khan, S.U.; Nasir, M.; Nawaz, M.H.; Niu, L. Functionalized graphene oxide bridging between enzyme and Au-sputtered screen-printed interface for glucose detection. *ACS Appl. Nano Mater.* **2019**, *2*, 1589–1596. [CrossRef]

154. Pilas, J.; Selmer, T.; Keusgen, M.; Schöning, M.J. Screen-printed carbon electrodes modified with graphene oxide for the design of a reagent-free NAD+-dependent biosensor array. *Anal. Chem.* **2019**, *91*, 15293–15299. [CrossRef]

155. Mazurenko, I.; Tananaiko, O.; Biloivan, O.; Zhybak, M.; Pelyak, I.; Zaitsev, V.; Etienne, M.; Walcarius, A. Amperometric Biosensor for Choline Based on Gold Screen-Printed Electrode Modified with Electrochemically-Deposited Silica Biocomposite. *Electroanalysis* **2015**, *27*, 1685–1692. [CrossRef]

156. Kim, J.; Imani, S.; de Araujo, W.R.; Warchall, J.; Valdés-Ramírez, G.; Paixão, T.R.; Mercier, P.P.; Wang, J. Wearable salivary uric acid mouthguard biosensor with integrated wireless electronics. *Biosens. Bioelectron.* **2015**, *74*, 1061–1068. [CrossRef] [PubMed]

157. Apetrei, I.M.; Apetrei, C. The biocomposite screen-printed biosensor based on immobilization of tyrosinase onto the carboxyl functionalised carbon nanotube for assaying tyramine in fish products. *J. Food Eng.* **2015**, *149*, 1–8. [CrossRef]

158. Rungsawang, T.; Punrat, E.; Adkins, J.; Henry, C.; Chailapakul, O. Development of Electrochemical Paper-based Glucose Sensor Using Cellulose-4-aminophenylboronic Acid-modified Screen-printed Carbon Electrode. *Electroanalysis* **2016**, *28*, 462–468. [CrossRef]

159. Bilgi, M.; Ayranci, E. Biosensor application of screen-printed carbon electrodes modified with nanomaterials and a conducting polymer: Ethanol biosensors based on alcohol dehydrogenase. *Sens. Actuators B Chem.* **2016**, *237*, 849–855. [CrossRef]

160. Hernández-Ibáñez, N.; García-Cruz, L.; Montiel, V.; Foster, C.W.; Banks, C.E.; Iniesta, J. Electrochemical lactate biosensor based upon chitosan/carbon nanotubes modified screen-printed graphite electrodes for the determination of lactate in embryonic cell cultures. *Biosens. Bioelectron.* **2016**, *77*, 1168–1174. [CrossRef]

161. Chen, D.; Liu, Z.; Fu, J.; Guo, Y.; Sun, X.; Yang, Q.; Wang, X. Electrochemical acetylcholinesterase biosensor based on multi-walled carbon nanotubes/dicyclohexyl phthalate modified screen-printed electrode for detection of chlorpyrifos. *J. Electroanal. Chem.* **2017**, *801*, 185–191. [CrossRef]

162. Hatada, M.; Tsugawa, W.; Kamio, E.; Loew, N.; Klonoff, D.C.; Sode, K. Development of a screen-printed carbon electrode based disposable enzyme sensor strip for the measurement of glycated albumin. *Biosens. Bioelectron.* **2017**, *88*, 167–173. [CrossRef]

163. Yang, P.; Peng, J.; Chu, Z.; Jiang, D.; Jin, W. Facile synthesis of Prussian blue nanocubes/silver nanowires network as a water-based ink for the direct screen-printed flexible biosensor chips. *Biosens. Bioelectron.* **2017**, *92*, 709–717. [CrossRef]

164. Salazar, P.; García-García, F.J.; González-Elipe, A.R. Sensing and biosensing with screen printed electrodes modified with nanostructured nickel oxide thin films prepared by magnetron sputtering at oblique angles. *Electrochem. Commun.* **2018**, *94*, 5–8. [CrossRef]

165. Vukojević, V.; Djurdjić, S.; Ognjanović, M.; Antić, B.; Kalcher, K.; Mutić, J.; Stanković, D.M. RuO$_2$/graphene nanoribbon composite supported on screen printed electrode with enhanced electrocatalytic performances toward ethanol and NADH biosensing. *Biosens. Bioelectron.* **2018**, *117*, 392–397. [CrossRef] [PubMed]

166. Bilgi, M.; Ayranci, E. Development of amperometric biosensors using screen-printed carbon electrodes modified with conducting polymer and nanomaterials for the analysis of ethanol, methanol and their mixtures. *J. Electroanal. Chem.* **2018**, *823*, 588–592. [CrossRef]

167. Cunha-Silva, H.; Arcos-Martinez, M.J. Dual range lactate oxidase-based screen printed amperometric biosensor for analysis of lactate in diversified samples. *Talanta* **2018**, *188*, 779–787. [CrossRef]

168. Cerrato-Alvarez, M.; Bernalte, E.; Bernalte-García, M.J.; Pinilla-Gil, E. Fast and direct amperometric analysis of polyphenols in beers using tyrosinase-modified screen-printed gold nanoparticles biosensors. *Talanta* **2019**, *193*, 93–99. [CrossRef]

169. Bilgi, M.; Sahin, E.M.; Ayranci, E. Sensor and biosensor application of a new redox mediator: Rosmarinic acid modified screen-printed carbon electrode for electrochemical determination of NADH and ethanol. *J. Electroanal. Chem.* **2018**, *813*, 67–74. [CrossRef]

170. Salazar, P.; Martín, M.; González-Mora, J.L. In situ electrodeposition of cholesterol oxidase-modified polydopamine thin film on nanostructured screen printed electrodes for free cholesterol determination. *J. Electroanal. Chem.* **2019**, *837*, 191–199. [CrossRef]

171. Maity, D.; Minitha, C.; RT, R.K. Glucose oxidase immobilized amine terminated multiwall carbon nanotubes/reduced graphene oxide/polyaniline/gold nanoparticles modified screen-printed carbon electrode for highly sensitive amperometric glucose detection. *Mater. Sci. Eng. C* **2019**, *105*, 110075. [CrossRef] [PubMed]

172. Aller-Pellitero, M.; Fremeau, J.; Villa, R.; Guirado, G.; Lakard, B.; Hihn, J.-Y.; del Campo, F.J. Electrochromic biosensors based on screen-printed Prussian Blue electrodes. *Sens. Actuators B Chem.* **2019**, *290*, 591–597. [CrossRef]

173. Uribe, P.A.; Ortiz, C.C.; Centeno, D.A.; Castillo, J.J.; Blanco, S.I.; Gutierrez, J.A. Self-assembled Pt screen printed electrodes with a novel peroxidase Panicum maximum and zinc oxide nanoparticles for H_2O_2 detection. *Colloids Surf. A Physicochem. Eng. Asp.* **2019**, *561*, 18–24. [CrossRef]

174. Erden, P.E.; Erdoğan, Z.Ö.; Öztürk, F.; Koçoğlu, İ.O.; Kılıç, E. Amperometric biosensors for tyramine determination based on graphene oxide and polyvinylferrocene modified screen-printed electrodes. *Electroanalysis* **2019**, *31*, 2368–2378. [CrossRef]

175. Arduini, F.; Cinti, S.; Caratelli, V.; Amendola, L.; Palleschi, G.; Moscone, D. Origami multiple paper-based electrochemical biosensors for pesticide detection. *Biosens. Bioelectron.* **2019**, *126*, 346–354. [CrossRef] [PubMed]

176. Jirakunakorn, R.; Khumngern, S.; Choosang, J.; Thavarungkul, P.; Kanatharana, P.; Numnuam, A. Uric acid enzyme biosensor based on a screen-printed electrode coated with Prussian blue and modified with chitosan-graphene composite cryogel. *Microchem. J.* **2020**, *154*, 104624. [CrossRef]

177. Castrovilli, M.C.; Bolognesi, P.; Chiarinelli, J.; Avaldi, L.; Cartoni, A.; Calandra, P.; Tempesta, E.; Giardi, M.T.; Antonacci, A.; Arduini, F. Electrospray deposition as a smart technique for laccase immobilisation on carbon black-nanomodified screen-printed electrodes. *Biosens. Bioelectron.* **2020**, *163*, 112299. [CrossRef]

178. Gomes, N.O.; Carrilho, E.; Machado, S.A.S.; Sgobbi, L.F. Bacterial cellulose-based electrochemical sensing platform: A smart material for miniaturized biosensors. *Electrochim. Acta* **2020**, *349*, 136341. [CrossRef]

179. Shitanda, I.; Mitsumoto, M.; Loew, N.; Yoshihara, Y.; Watanabe, H.; Mikawa, T.; Tsujimura, S.; Itagaki, M.; Motosuke, M. Continuous sweat lactate monitoring system with integrated screen-printed MgO-templated carbon-lactate oxidase biosensor and microfluidic sweat collector. *Electrochim. Acta* **2021**, *368*, 137620. [CrossRef]

180. Brenes, J.P.; Arroyo-Mora, L.E.; Barquero-Quirós, M. Enzymatic inhibitive determination of AB-Fubinaca and AB-Pinaca on screen printed carbon tetratiofulvalene electrodes modified with nanoparticles and carbon nanotubes. *Sens. Bio-Sens. Res.* **2022**, *38*, 100515. [CrossRef]